DEPARTMENT OF INDUSTRIAL MANAGEMENT AND TECHNOLOGY, UNIVERSITY OF PIRAEUS

SCHOOL OF CHEMICAL ENGINEERING, NATIONAL TECHNICAL UNIVERSITY OF ATHENS

ADMINISTRATION AND MANAGEMENT OF INDUSTRIAL SYSTEMS

SPECIALIZATION: SYSTEMS OF ENERGY AND ENVIRONMENTAL MANAGEMENT

Biosensors for the Control of Environmental Parameters

Olga Mermigka

Board
C. Siontorou (Supervisor)
F. Batzias
D. Sidiras

Piraeus 2012

Acknowledgements

First of all, I would like to express my gratitude to Professor F. Batzias who gave me the opportunity to work in his lab "Simulation of Industrial Processes" and enabled my studies and research activities.

A very special debt of gratitude I owe to Lecturer C. Siontorou for the continuous scientific guidance and the entire support and help, she offered me for the time she was my supervisor.

I would also like to thank Associate Professor D. Sidiras for offering his precious advice whenever I needed it.

I also owe very special thanks to the rest of the team in the lab for a great working atmosphere and all our social activities.

Finally, I would want to thank my family and my friends that support me in my effort.

Summary

This work presents the design/development of biosensors based on metal supported bilayer lipid membranes (s-BLMs), intended for the qualitative and quantitative detection of substances of environmental interest. Biosensor design proceeds through a knowledge-based approach that takes into consideration environmental constraints, needs, and parameters, followed by analytical development and validation. Two case examples are presented: (i) polycyclic aromatic hydrocarbons (PAHs) monitoring in estuarine areas, and (ii) hyperoxide-based detection. The former is used to illustrate the functionality of the knowledge-based design, whereas the latter follows analytical development protocols (construction, physicochemical characterization, performance evaluation). The hyperoxide sensor was built on egg phosphatidylcholine (egg PC) membranes incorporated with horseradish peroxidase, whereas two immobilization techniques have been tested: physisorption of the enzyme at the pre-formed bilayer and addition of the enzyme into the lipid forming mixture prior to BLM self-assembly. The sensor has been validated using commercial hyperoxide formulations. The results indicate that hyperoxide can be rapidly screened using the present metal-supported BLM-based minisensor. The approach provides response times of seconds and detection sensitivity and limits for hyperoxide that are suitable for direct analysis of industrial or environmental samples without preconcentration (although sample preparation to eliminate other adsorbents to BLMs may be necessary). While the work presented here represents an attractive configuration and application of electrochemistry of BLM-based sensors, the practical use of such a sensor for real world applications needs to be further researched for robustness, lifetime, manufacturability, and other performance requirements that will further allow commercialization of the present device.

Περίληψη

Η παρούσα εργασία αναφέρεται στο σχεδιασμό και την ανάπτυξη βιοαισθητήρων διστρωματικών λιπιδικών μεμβρανών υποστηριζόμενων σε ακροφύσια ηλεκτροδίων (metal supported bilayer lipid membranes — s-BLMs), για τον ποιοτικό και ποσοτικό προσδιορισμό ουσιών περιβαλλοντικού ενδιαφέροντος. Για το σχεδιασμό του βιοαισθητήρα χρησιμοποιείται έμπειρο σύστημα προκειμένου να προσδιορισθούν οι περιορισμοί, ανάγκες και παράμετροι του περιβάλλοντος λειτουργίας και, εν συνεχεία, κατασκευάζεται σε εργαστηριακή κλίμακα και αξιολογείται. Παρουσιάζονται δύο παραδείγματα: (i) ανίχνευση πολυκυκλικών αρωματικών υδρογονανθράκων (polycyclic aromatic hydrocarbons — PAHs) σε εκβολές ποταμών και (ii) ανάλυση που βασίζεται στην ανίχνευση υπεροξειδίου. Ο σχεδιασμός βιοαισθητήρα για την παρακολούθηση των PAHs παρουσιάζει τη λειτουργικότητα του μεθοδολογικού πλαισίου και του έμπειρου συστήματος, ενώ ο βιοαισθητήρας υπεροξειδίου ακολουθεί τα πρωτόκολλα αναλυτικής ανάπτυξης (κατασκευή, φυσικοχημικός χαρακτηρισμός, αξιολόγηση). Ο αισθητήρας υπεροξειδίου κατασκευάσθηκε με λιπιδικές μεβράνες φωσφατιδυλοχολίνης αυγού (egg phosphatidylcholine — egg PC) στις οποίες ακινητοποιήθηκε/ενσωματώθηκε υπεροξειδάση αγριοραπανίδας (horseradish peroxidase — HRP). Αξιολογήθηκαν δύο τεχνικές ακινητοποίησης: (α) φυσική προσρόφηση σε σχηματισμένη λιπιδική μεμβράνη και (β) προσθήκη του ενζύμου στο διάλυμα λιπιδίων πριν την έναρξη της διαδικασίας σχηματισμού της μεμβράνης. Ο βιοαισθητήρας αξιολογήθηκε σε εμπορικά σκευάσματα υπεροξειδίου. Τα αποτελέσματα δεικνύουν ότι ο μικρο-αισθητήρας λιπιδικών μεμβρανών που κατασκευάσθηκε παρέχει μικρούς χρόνους απόκρισης (της τάξεως των s), ικανοποιητική ευαισθησία και μικρό όριο ανίχνευσης, χωρίς να απαιτείται η συμπύκνωση του δείγματος (παρ' ότι πιθανόν να απαιτείται προκατεργασία του δείγματος προκειμένου να απομακρυνθούν άλλες παρεμποδίζουσες ουσίες που περιέχονται στο δείγμα). Όπως προκύπτει, το σύστημα ηλεκτροχημικής ανίχνευσης με μεμβρανικούς βιοαισθητήρες είναι κατάλληλο για την παρακολούθηση περιβαλλοντικών ρυπαντών, η εφαρμοσιμότητά του, όμως, απαιτεί περαιτέρω μελέτη ως προς την ευρωστία, το χρόνο ζωής, τη δυνατότητα παραγωγής και άλλες παραμέτρους, οι οποίες ορίζουν την εμπορευματοποίηση της συσκευής.

Table of Contents

1. Biosensors for environmental monitoring

1.1 Introduction

The increasing awareness of the scale of environmental problems has brought attention on the urgent need for sensitive and analytically precise diagnostic tools with a predictive capability in pollution impact assessment. This goal can only be achieved through an improved mechanistic understanding of the perturbations induced by toxic contaminants. Such knowledge will lead to the development of conceptual frameworks linking impact at the molecular level to consequences at the cellular and higher levels of biological organization.

The monitoring of biological responses to pollution (biotic effect) rather than the pollution itself (abiotic pattern) draws a new strategy in environmental assessment. The level of pollutants detected in the tissues of organisms is the only direct measure of the proportion of the total toxicant delivery to biota, and therefore indicates the fraction that is likely to enter and affect the ecosystem. Numerous approaches, such as biomonitoring, biosensing, biological treatment and bioremediation, have been linked to this concept [1-3], without however been successful in coupling site-derived stress response mechanisms and site-relevant information within a single format. Biomonitoring surveys evaluate the status of the local ecosystem (i) at a site-relevant phenomenological level, relying on metrics and indices that cannot satisfy deeper knowledge levels, (ii) at cellular level by chemical analysis giving, however, no information on species synergy, and (iii) at sub-cellular level by lab-based fumigation studies, that serve well the elucidation of dose-response relations, being, however, neither site-derived or site-relevant [1]. Biological treatment and bioremediation techniques rarely utilize indigenous flora and fauna, balancing dangerously between treatment optimization and ecosystem perturbation [2]. Biosensors fuse successfully natural chemoreception to transducers for chemical analysis through a design approach that rarely takes into consideration local biogeochemical characteristics, thus compromising reliability of *in situ* measurements [3].

Evidently, it is necessary to explore and apply new approaches to environmental assessment, combining both biological responses and chemical analysis, to identify toxic hotspots, to characterize chemicals likely to cause adverse biological effects,

and, finally, to assess the ecological risk of the identified chemicals at relevant spatial scales.

1.2 The concept of Biosensor

1.2.1 Definition

A biosensor can be defined as an analytical device incorporating a biological sensing element, either intimately connected or integrated to a physicochemical transducer or transducing microsystem [4]. The aim of a biosensor is to detect a chemical moiety in a complex sample. The mode of operation is similar to natural chemoresception, i.e., biosensors utilize a biological system (either single, as, for example, an enzyme or an antibody, or more complex, as for example DNA or a whole cell) that selectively interacts with the chemical moiety (serving, respectively, as the substrate, the antigen, an adduct or a metabolic substance) producing a biological signal (either as reaction yield, complex formation, perturbation, conformational change, etc.) that is translated into a digital electronic signal by the transducer.

The biological components of the biosensor, i.e., the sensing components or the bioelements, can be divided into three distinct groups: behavioural, catalytic and noncatalytic. The behavioural group consists of living higher organisms (e.g. fish, mussels, etc.), the catalytic group includes enzymes, microorganisms and tissues, while the non-catalytic or affinity class comprises antibodies, receptors and nucleic acids [7].

The principal components of a biosensor and their functions can be seen in *Figure 1.1*, while the main performance characteristics of biosensors are described at *Table 1.1*. In general biosensors are classified either by their biological element or the transducer used. In some cases the immobilisation method used to attach the biological element to the transducer is used for classification (*Figure 1.2*). The combination of highly specific biological reactions with an appropriate transducer gives biosensors a number of advantages, such as the high sensitivity and specificity of the biological element. The resolution of biosensors is far superior to most chemical recognition systems, since, in theory, it is possible to detect a single molecule within a complex matrix. Biosensors also provide short response times and

in many cases allow real-time measurements. The nature of biosensors allows miniaturisation and integration into portable instruments, making biosensors an ideal choice for on-site measurements. The limits to miniaturization are essentially the miniaturization capability of the transduction system, as the bioelements already measure down to nanosizes.

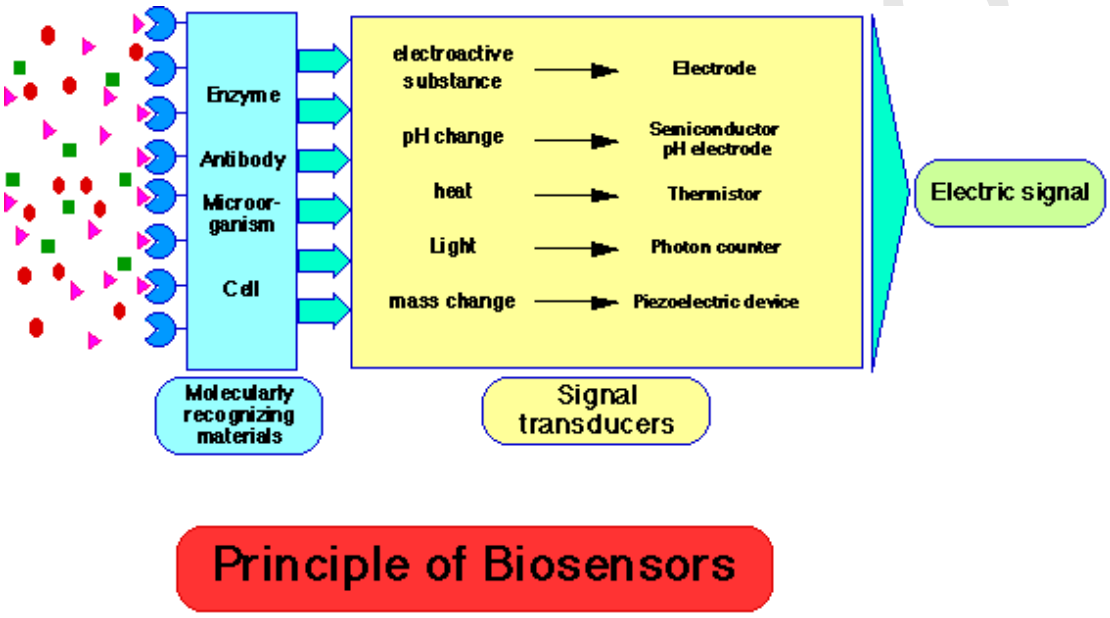

Figure 1.1: *Principle of a biosensor, adapted from [4].*

Table 1.1: *General performance characteristics of biosensors and terminology, adapted from [8]*

Term	Definition
Sensitivity	The slope of the response curve expressed as output per unit concentration.
Selectivity	The ability of the device to measure one chemical component in presence of others.
Dynamic Range	The range of concentrations in which the sensitivity is greater than zero.
Response Time	The time at which the output reaches 63% (1/e) of its final value in response to a step change in concentration.
Reproducibility	Accuracy, usually expressed as variance, standard deviation or coefficient of variation.
Detection Limit	The concentration at which the mean value of the output is equal to two standard deviations.
Life Time	The usable period of the biosensor, either as “shelf” or “in-use”.
Stability	The percent change of the baseline and/or sensitivity in time.

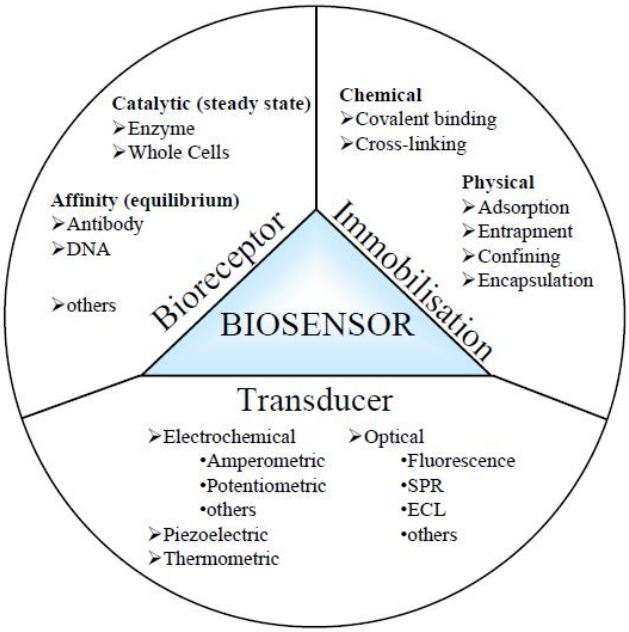

Figure 1.2: *Classification of biosensors by biocomponent, transducer and immobilisation method, adapted from [5].*

1.2.2 Transduction schemes

A transducer is a device that is activated by energy from one system and supplies energy, often in another form, to a second system [6]. In biosensors this means that energy produced directly or indirectly by a biological reaction is generally converted into an electrical signal.

The transduction technology includes electrochemical elements, which may be amperometric (the measurement of current flowing at constant potential), potentiometric (the measurement of potential changes at constant current) or conductimetric (the measurement of changes of conductivity between two electrodes); optical elements (the measurement of changes in optical properties, like absorption, fluorescence, light emission or reflection); acoustic/piezoelectric (the measurement of changes in the acoustic properties of the sensor, like biosensors based on piezoelectric materials); and calorimetric/thermal (the measurement of small changes in temperature) [7].

The nature of the biological element is the main determinant for the selection of the transducer. Enzymatic reactions are easily monitored, electrochemically, thermometrically or photometrically, whereas mass sensitive devices are usually not used for enzymatic biosensors. On the other hand, piezoelectric sensors can detect

affinity reactions of antigen and antibody or DNA without labelling [5]. Other transducers frequently require some sort of label for affinity measurements. *Table 1.2* shows the types of transdusers exploited in biosensors.

Table 1.2: *Types of transdusers exploited in biosensors [9].*

Transduser System	Measurement Mode	Typical Applications
1. Electochemical.		
(a) Conductimetric.	Conductance	Enzyme-catalysed reactions.
(b) Enzyme electrode.	Amperometric (current)	Enzyme substrates and immunological systems (antibody-antigen).
(c) Field effect transistors (FET).	Potentiometric (voltage)	Ions, gases, enzyme substrates and immunological analytes.
(d) Ion-selective electrodes (ISE).	Potentiometric (voltage)	Ions in biological media, enzyme electrodes, immunoelectrodes.
(e) Gas-sensing electrodes.	Potentiometric (voltage)	Gases, enzymes, organelle, cell or tissue electrodes, enzyme immunoelectrodes.
(f) Impedimetric.	Impendance	Enzyme immunosensors.
2. Piezo-electric crystals, surface acoustic devices.	Mass change	Volatile gases, vapours and immunological analytes.
3. Optoelectronic, fibre optics and waveguide devices.	Optical	pH, enzyme substrates, immunological analytes.
4. Thermistors, diodes.	Thermometry/calorimetric (heat)	Enzyme, organelle, whole cell or tissue sensors for substrates, gases, pollutants, antibodies, vitamins, immunological analytes.

1.2.2.1 Electrochemical Biosensors

Owing to its well established use, electrochemical transduction constitutes a successful route to create low-cost biosensors when coupled to enzymes. However, electrochemical detection of just a biorecognition process is difficult. Catalysis leading to the formation of electroactive substances is frequently necessary. Electrochemical sensors may work under amperometric, potentiometric, conductimetric and impedimetric transducing principles.

For amperometric devices the current generated by oxidation or reduction of redox species at the electrode surface maintained at the appropriate electrical potential is measured [10]. The current observed has a linear relationship with the

concentration of the electroactive species. In potentiometric biosensors changes in potential after the specific binding of the target to the immobilized partner, under zero-current conditions, are detected [10]. Conductimetric and impedimetric biosensors are essentially based on the same physical principle. Conductimetry describes the dependence of the current generated by ions in solution while impedance refers to the voltage as a function of the current [10]. In both cases, the conductimetric or impedimetric properties are influenced by a sensing layer placed between the two electrodes [10].

1.2.2.2 Piezoelectric/Acoustic Biosensors

Within mass-sensitive biosensors, acoustic wave biosensors operate on the basis of an oscillating crystal that resonates at a fundamental frequency. The crystal element is coated with a layer containing the biorecognition element designed to interact selectively with the target analyte [10]. Piezo-electric biosensors are principally based on the measurement of change in resonant frequency of a piezo-electric crystal as a result of mass changes on its surface [9]. In principle, two waveforms are used for piezoelectric biosensors. One is a surface acoustic wave (SAW) device and the other bulk acoustic wave (BAW) device, which is most commonly used [5].

1.2.2.3 Optical Biosensors

First developments of these kinds of sensors took advantage of the flexibility and low cost of the optical fibres measuring the absorption or emission of light of one of the components of the bioreaction [10]; that gave rise to optrodes. Apart from speed, sensitivity and robustness, other attractive features of optical sensors include their suitability to component miniaturization, remote sensing and their multi-analyte sensing capabilities [10]. The main disadvantage of optical sensing is the light interference, which raises substantially the detection limits.

In optical biosensors different techniques can be employed by using evanescent waves (EWs), surface plasmon resonance (SPR), which is actually a hybrid between piezoelectric and optical sensing, and electrochemiluminescent (ECL) [5].

1.2.2.4 Calorimetric biosensors

The enzyme thermistor has demonstrated the possibility of using calorimetric techniques for biochemical detection [11]. Thermometric biosensors exploit the change of heat, absorption or evolution, which occurs during biochemical reactions. This heat fluctuation is reflected in a change of temperature within the reaction medium [5]. Sensitive thermistors are used to monitor the temperature change.

1.2.3 The range of bioelements

The biological components of biosensors are not only responsible for the selective recognition of the analyte, but also the generation of the physico-chemical signal monitored on the transducer and, ultimately, the sensitivity and the shelf- or in-use life of the final device [12].

The sensing element in a biosensor is a highly specific bioreceptor. Compared to most chemical sensing elements, these bioreceptors show remarkable specificity towards one particular analyte or a family (group) of analytes. Over the years, a number of different biological elements have been used in biosensors. The most important bioelements for biosensors are enzymes with their specificity towards certain substrates. Also important is the biorecognition between antibody and antigen, as used for immunological sensors. Other biomolecules frequently used are DNA strands with affinity towards complementary strands or other molecules [5]. Other systems include whole cells, bacteria, yeasts, subcellular fractions, membrane receptors and tissue slices.

Depending on their biological element, biosensors can be catalytic sensors or affinity sensors [5]. In catalytic sensors, an enzymatic reaction often involving the analyte, causes the concentration change of a detectable compound. In affinity sensors, the binding between the analyte and receptor is monitored, e.g. with antibodies or DNA.

The catalytic group includes enzymes, microorganisms and tissues [12]. Devices incorporating these elements are appropriate for monitoring metabolites in the millimolar to micromolar range and can be used for continuous monitoring. The non-catalytic or affinity class biological component comprises antibodies (or antigens), lectins, receptors and nucleic acids which are more applicable to 'single use' disposable devices for measuring hormones, steroids, drugs, microbial toxins, cancer markers and viruses at concentrations in the micromolar to picomolar range [12].

More recently, a hybrid configuration of biosensor has been introduced which combines the attributes of both the high affinity ('irreversible') binding of an antibody or DNA/RNA probe with the amplification characteristics of an enzyme [12]. These systems are capable of monitoring analytes in the picomolar to attomolar concentration range and lower.

Biomolecules and biological systems of relevance to biosensor research may be divided into the following main groups [13]:

a) enzymes: proteins which catalyse specific biochemical transformations,
b) antibodies: globular serum proteins (known as immunoglobulins, Ig) which form an important part of a much wider biological group termed binding proteins. Antibodies bind a particular substance (the corresponding antigen) with high specificity and high affinity,
c) whole cells: intact biological structural units which contain a wide range of biomolecules and which respond to many types of chemicals,
d) receptors: protein systems which interact with specific chemicals such as hormones with a resultant conformational change, and
e) tissues: tissue systems, deriving mainly from insects (antennas), that already possess the sensing elements attached, interact with specific analytes, and give signals partly utilizing the embedded signal transmission system.

1.2.3.1 Catalytic Bioreceptors

1.2.3.1.1 Enzymes

Enzymes are proteins (polypeptide structures) acting as biological catalysts responsible for most chemical reactions in living organisms. Their main task is to initiate or accelerate reactions that would otherwise not take place, or only very slowly, at the moderate temperatures predominant in organisms without being consumed in the process [13, 5]. They also slow down reactions, if necessary, or split them up into separate steps, to control the heat evolution of exothermic reactions. Otherwise, the uncontrolled heat evolution could lead to cell death.

Enzymes are found in all types of cells; a given cell will typically contain many hundreds of enzymes, though the exact distribution and quantity of enzymes present varies considerably according to the cell's natural function [13].

Enzymes are the most commonly used biocatalysts in biosensors. Electrochemical biocatalytic sensors using enzymes have dominated the biosensor market for years

with oxi-reductases being the most important enzymes (e.g. glucose oxidase) [5]. Some enzymes such as urease are highly specific for one compound. Other enzymes on the other hand, are specific for a whole group of substrates.

The structure of individual enzymes varies immensely within the basic framework of a polypeptide structure and determines the catalytic role of the molecule [13]. The 3-dimensional structure of an enzyme is formed by the relatively complex and highly precise folding of a single polypeptide chain. Within this structure there is a small portion, typically defined by a group of 5 - 10 amino acids spatially arranged in a specific relative conformation, which interacts with the substrate (S) of the enzyme (E) during E-S transition state complexation [13]. This region of the enzyme molecule is known as the active site (or catalytic site).

Only certain molecules are allowed access to the active site, so that the specificity of the enzyme is mainly determined by access through the protein shell and the binding site, and not by the active site itself [5].

The active site of many enzymes is located in the interior of the protein structure to promote specificity towards the substrate, and to reduce non-specific interactions and access to inhibitor molecules. Certain enzymes possess one or more additional active areas defined by specific amino acid arrangements which may bind a subsequent reactant or a co-factor. A co-factor is a non-protein organic chemical that is required to achieve maximum efficiency in the enzymatic catalysis (for example, NADH). The active site of an enzyme is designed by evolution to facilitate chemical transformation of the substrate by promoting redistribution of electron density within the substrate molecule through the formation of ionic or hydrogen bonding interactions [13]. Hydrophobic forces are also believed to play a role in E-S complexation.

When the substrate (S) binds to the binding site of the enzyme (E), a reactive intermediate, the enzyme substrate complex (ES) is formed. The complex ES is converted to E and a product (P) by the active site. Whereas the complex formation step is reversible, the product forming step with the rate constant k_2 can be considered irreversible, since the affinity of the enzyme towards P is generally negligible [5].

Activators, such as metal ions, may interact with the enzyme or E-S complex to facilitate reaction in certain enzymatic systems. The energy required to attain the intermediate transition state in the reaction is substantially lowered as a result of interactions (e.g. hydrophobic forces); this, in turn, results in a more rapid rate of

reaction [13]. Conversion of the E-S complex to product (P) is followed by dissociation of P from the active site to regenerate reactive enzyme. The rate at which the enzyme converts S to P is reflected in the enzymatic activity, which is defined as the amount of substrate S converted to product P per unit weight of enzyme per unit time under defined conditions (for example, pH, temperature) [13]. A similar parameter is the 'turnover number' of the enzyme which is defined as the number of substrate molecules transformed per molecule of enzyme per second. Under suitable conditions, enzymes are very stable and can work for weeks or months with very high turnover rates. One single enzyme can convert between 10^3 and 10^8 substrate molecules per minute [5].

During enzymatic reactions, substrates are consumed and products formed. These compounds can be monitored with suitable transducers. For example, the glucometer, i.e., the biosensor used for measuring the levels of blood glucose in diabetic patients, utilises the product formed by the oxidation of glucose or the consumption or oxygen during oxidation.

There are two main applications for enzymes in biosensors. They can either be used as catalytic biosensors or as markers in affinity biosensors, such as immunosensors and DNA sensors.

In catalytic enzyme sensors, the concentration of enzyme [E] is constant and the substrate concentration [S] is much smaller [5]. The velocity ν is only dependent on the substrate concentration.

When the enzyme is used as a label for antibodies or DNA strands, the substrate must be used in excess and the enzyme concentration [E] is the only limiting factor. The reaction is of first order for the enzyme concentration.

Since enzymes can convert hundreds of substrate molecules per second, they are highly efficient chemical amplifiers for the detection of other molecules.

Enzymes are sensitive to temperature changes. Increasing temperatures increase the reaction rate, but at elevated temperatures, the protein structure (tertiary structure) denatures, mostly irreversible, leaving the enzyme inactive [5]. For most enzymes, this critical temperature starts between 40°C and 50°C, however, few enzymes can possess high thermal stability above 100°C. Enzymes consist of amino acids and are therefore sensitive to pH [5].

Enzyme reactions can be inhibited by various species. Inhibition may be reversible, allowing the enzyme to regain full activity after dissociation from the

inhibitor. These inhibitors can competitively block the active site or alter the enzyme activity by other mechanisms. Other inhibitors inhibit the enzyme and deactivate it irreversibly. These irreversible inhibitors can work in different ways, for example blocking the binding site, reacting with the central metal ion or denaturing the enzyme [5]. Enzyme inhibition sensors have been reported for the detection of toxic compounds and heavy metal ions and are based on the selective inhibition of enzymes.

1.2.3.1.2 Whole cells

Biological cells are small membrane-bounded structures which contain a high concentration of chemicals including enzymes, nucleic acids, ions, and many different types of protein, small organic molecules and many others. The simplest living cellular systems are unicellular algae or bacteria where the entire organism consists of a single cellular unit (*Figure 1.3*).

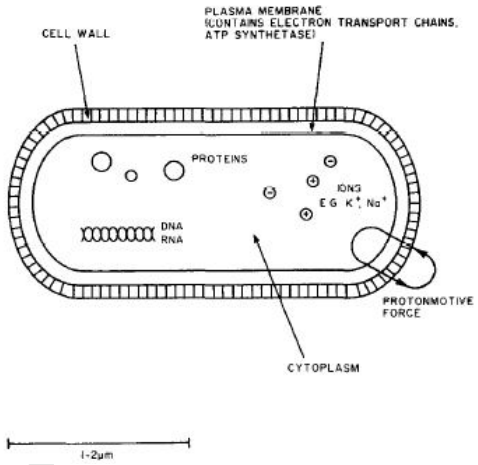

Figure 1.3: *Basic structure and main components of a typical bacterial cell [13].*

In higher organisms many billions of cells are present, each of which has a specific function governed by the genetic code of the organism. The complexity of a cell, both structural and chemical, confers sensitivity to an extremely wide range of compounds.

However, individual types of cell can demonstrate a particular set of physico-chemical or biological changes in response to a specific type or group of chemicals. The sensitivity and specificity of a particular cell for a particular chemical varies enormously depending on the type, source, and environment of the cell and the exact nature of the chemical itself [13].

The stability of biological cells is of critical importance for biosensor applications. In general, cells derived from higher organisms are more difficult to isolate and maintain in a viable form for the extended periods of time required in most sensor formats [13].

1.2.3.2 Affinity Bioreceptors

1.2.3.2.1 Antibodies

Antibodies are produced by mammals as part of an immune response of the host to foreign intruders. The immune system specifically recognises and eliminates pathogens. The first line of defence is innate immunity, a non-specific defence reaction. More important for analytical science is the second line of defence, adaptive immunity. Adaptive immunity is directed specifically against the intruder and is mediated by cells called lymphocytes [5].

Antibodies are serum proteins which are produced by two types of blood cells, B lymphocytes and plasma cells, in response to a foreign (nonself) substance [13]. The foreign substance is termed an immunogen, so-defined because it evokes an immune response (that is, production of many antibodies). The antigen - antibody reaction may be regarded as highly specific.

Antibodies (also referred to as immunoglobulins, Ig) consist of four polypeptide sub-units comprising two identical large or heavy chains (H chains) and two identical small or light chains (L chains) which are held together by non-covalent forces and covalent interchain disulphide bonds [13]. The carbohydrate residues in antibodies are covalently bonded to the C-terminal half (Fc) of the molecule and have a function that is not yet fully determined.

The key portions of the antibody molecule that contain the antigen binding sites are termed the Fab fragments; each Fab fragment comprises an entire light chain and a segment of the heavy chain. Fab fragments are often used for biosensor applications because of a number of potential advantages over whole Ig molecules including [13]:

- reduction of non-specific binding, as Ig molecules contain Fc portions which are ‘sticky’ towards non-antigenic components in the sample,
- a preparative route which degrades interferent non-antibody proteins present in serum which could also bind antigen,

- a single antigen binding site in contrast to two sites on Ig molecules (this prevents the formation of antigen-bridged complexes which distort conventional quantitation methods in immunoassays),
- greater control over the stereochemistry of immobilization through use of -SH groups produced from cleavage of disulphide (S-S) bonds during Fab fragment preparation.
- Antibodies have been used very widely in laboratory-based immunoassays for detection of an extensive range of individual single analytes, each one of which must be, of course, the corresponding antigen of the antibody used in the test. Antibodies cannot be synthesized by chemical means; they can only be obtained by inducing the generation of the required antibody using an animal species with a well-developed immune-system, normally, a mammal.

The region of an antigen that interacts with the antibody binding site (paratope) is called the epitope [5]. This means that epitopes are not intrinsic parts of the molecule. The actual part of the antigen molecule that acts as an epitope can vary from one antibody to another for exactly the same molecule. Antibody antigen interactions are reversible and non-covalent and involve hydrogen bonds, van der Waals forces, ionic coulombic interactions and hydrophobic bonds. Both, antigen and antibody can undergo substantial conformational changes upon interaction, but they may also stay unchanged, depending on the specific antibody antigen pair.

The specifications of immunosensors are determined to a large extent by the affinity of their components. High affinity results in sensitive sensors, but too high affinities might result in virtually irreversible sensors.

Avidity is the measure of the overall stability of the antibody antigen complex. For immunochemical reactions, avidity is of more practical importance than affinity, because it refers to intrinsic affinity of the paratope for the epitope, the valency of the antibody and the geometric arrangement of the interacting compounds [5]. High avidity is reached when all paratopes can bind epitopes.

The two major problems with antibodies in immunosensors are the requirement to be fully reversible in a short period of time and the efficient transduction of the antibody antigen binding event into a usable signal. Compared to enzymes, antibodies have higher affinity constants and the antibody antigen interaction is of a more long-term nature. With an enzyme, the substrate is converted to a product which is then

ejected due to low affinity [5]. New substrate can access the enzyme straight away, resulting in a very fast process. In the case of enzyme labels, this process results in signal amplification. Substrates or products can often be directly detected. Antibody and antigen form a very stable complex and although the interaction is reversible, even intensive washing can often fail to dissociate the complex in a reasonable time [5]. Often, special agents have to be used to release the antigen.

Another disadvantage is that the antibody antigen interaction produces no detectable product and is difficult to monitor directly. Only a few transducers are able to detect the interaction directly (label-free). Most reported immunosensors, however, are based on indirect assays, often competition and inhibition, with easily detectable labels such as enzymes, fluorophores and redox molecules.

Disposable immunosensors can be mass produced and are inexpensive and easy to use.

1.2.3.2.2 Receptors

Molecular receptors are cellular proteins (often membrane-bound) which bind specific chemicals in a manner which results in a conformational change in the protein structure. The conformational change triggers a cellular response. In general, molecular receptors are distinct from receptors (which include larger multi-component systems) on the basis of their composition, which is a single protein structure, though possibly containing more than one subunit [13].

Molecular receptors have two important properties relevant to their possible incorporation into biosensor devices, namely their intrinsic signal amplification properties and their high specificity. The former are a direct result of the biochemical consequences triggered by even a single receptor-ligand interaction. The latter advantage, ligand specificity, is a consequence of the highly evolved binding region of the receptor which is fully optimized for binding the particular ligand.

Major limitations in the studies and use of molecular receptors are [13]:

- the relatively difficult experimental procedures necessary to isolate the receptor proteins (even prior to purification) which are both time-consuming and expensive, in addition to requiring, in many cases, animal sources,
- the inability, at present, to obtain more than very small amounts of pure receptor, and

– the rapid loss of biological function which follows isolation in most cases.

Comparatively few biosensors of this type have been reported, primarily because of the problems associated with successful isolation of molecular receptors (in sufficient quantities and purity) and stabilization of these molecules in artificial environments such that appreciable biological activity is retained [13].

1.2.3.2.3 Nucleic Acids: DNA Biosensors

Biological elements used with growing interest in affinity biosensors are nucleic acids in the form of DNA or RNA. DNA biosensors consist of an immobilized DNA strand to detect the complimentary sequence by DNA–DNA hybridization [14]. Compared to enzyme biosensors and immunosensors, there is still a scarcity of DNA biosensors available in the market and/or under research and development. Unlike enzymes or antibodies, DNA forms biological recognition layers easily synthesizable, highly stable and reusable after simple thermal melting of the DNA duplex [14]. In general, the underlying mechanism of quantitative DNA detection through DNA biosensors is the highly specific hybridization between two complimentary DNA chains which, unlike in conventional solid-state hybridization formats, occurs directly on the surface of a physical transducer [14].

The first and more obvious possibility single stranded DNA (ssDNA) offers, is the detection of complementary strands. A specific oligo nucleotide is immobilised on a surface and the hybridisation reaction can be monitored with a suitable transducer [5]. The second sensing system using DNA is somewhat different. Here the affinity of certain small organic molecules towards nucleic acids is used for sensing. These molecules are able to intercalate ssDNA or double stranded DNA (dsDNA) [5]. The guanine peak of the immobilised DNA can be measured electrochemically. This signal changes upon intercalation. Compounds measured with such a system include PCBs, PAHs, aromatic amines and aflotoxin B1.

1.2.4 Immobilization techniques

The immobilisation of the biological element onto the transducer is very important for the biosensor performance. The optimal immobilisation method would yield a biomolecule immobilised on the surface of a transducer, retaining its full activity with long-term stability regarding its function and immobilisation. Furthermore, the

biomolecule should be fully accessible for substrate, analyte, co-reactant, antigen, antibody or oligonucleotide. The transducer should be unaffected by the immobilisation step. Many immobilisation methods can fulfil a number of these requirements, but they also have disadvantages. Therefore, the immobilisation method has to be chosen and adapted for the particular bio element, transducer, matrix and other assay requirements.

The most common immobilisation methods used for biosensors can be divided into physical and chemical methods (*Figure 1.4*) [5]. Physical methods include adsorption, entrapment, encapsulation and confining. The chemical method is covalent binding. However, cross-linking of biomolecules is also used to improve the stability of physical methods.

1.2.4.1 Physical methods

1.2.4.1.1 Physical Adsorption

Physical adsorption of biomolecules to solid surfaces is a simple technique. Many different surfaces are used for adsorbing biomolecules. These materials include cellulose, collagen, PVC, gold and carbon. The enzyme connection with the water soluble material takes place via ionic, polar or hydrophobic bonds, hydrogen bonds or via π-electron interactions. Proteins are attached to these surfaces by low energy bonds such as charge-charge interactions, hydrogen bonds, van der Waals forces and hydrophobic interactions [5].

The advantage of adsorption as an immobilisation method is its simplicity. Frequently, the surface is only incubated in the protein solution for a certain time and then washed to remove excess protein. However, the stability of the protein layer is generally poor and can be affected by many factors, such as pH, ionic strength or temperature. To improve the stability of the adsorbed molecules, they are sometimes cross-linked with bifunctional reagents such as glutaraldehyde. This results in an adsorbed network rather than adsorbed molecules [5]. Unfortunately, the process of cross-linking can deactivate the biomolecules to some extent.

Other techniques passively adsorb proteins, which are often used in disposable sensors and, where the protein layer is not reused and extended stability is not required to the same extent as in permanent or reusable sensors [5].

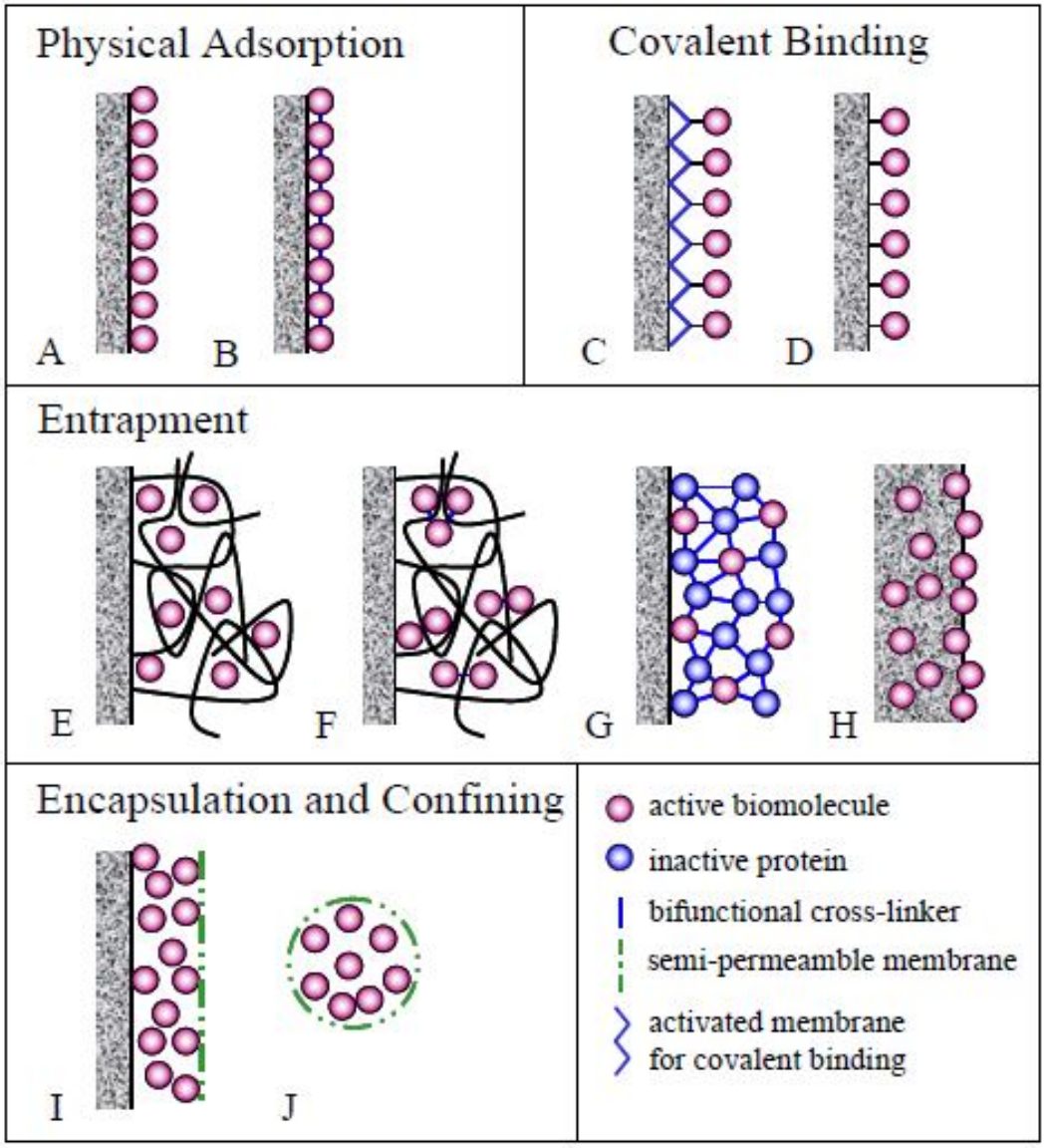

Figure 1.4: *Immobilization of the biological element: A) adsorption; B) adsorption with cross-linking; C) covalent binding on an activated membrane; D) covalent binding on an activated transducer surface; E) gel entrapment; F) gel entrapment with cross-linking; G) co-reticulation; H) entrapment in an electrode; I) confining with semi-permeable membrane; and J) spherical micro-encapsulation, adapted from[5].*

1.2.4.1.2 Entrapment

The biological element can be entrapped in a three dimensional polymeric lattice. This is normally achieved by forming a networked polymer gel around the biomolecule. Starch gels, silicate and polyacrylamide gels are frequently used. The network can be formed by polymerising a three dimensional structure or by cross-

linking two-dimensional polymer strands. Polymerisation is also carried out electrochemically.

The gel can also be formed with a technique called co-reticulation [5]. A mixture of excess of inactive protein, such as BSA, and the active biomolecule are crosslinked. The resulting network is a gel, formed by the cross-linked inactive protein with the active biomolecule trapped and cross-linked in the gel.

The biological element is homogeneously entrapped in the gel, but is often only accessible for small molecules. On the other hand, the irregular (heterogeneous) structure of the gel might cause leakage of the biomolecules from less densely polymerised regions [5]. Cross-linking of the molecules might overcome the problem and retain more biomolecules in the gel, but the bifunctional cross-linkers might also deactivate the biological elements. Damage or deactivation might also occur during polymerisation, depending on the mechanism and the conditions used.

Gel entrapment is a popular immobilisation method for whole cells, but not for antibodies or antigens. Whole cells are retained very well in the gel due to their size and their analytes and substrates are mostly small molecules. In immunogenic reactions, however, mainly large molecules are involved and as such cannot move freely through the gel.

Another form of entrapment is the incorporation of the biological element in the electrode matrix [5]. Enzymes for example can also be incorporated in composite electrodes. A mixture of graphite particles, enzymes and plastifier (water insoluble liquid or solid) forms the electrode. Direct incorporation of biomolecules is also possible when electrodes are screen-printed.

1.2.4.1.3 Encapsulation and Confining

Encapsulation and confining as an immobilisation method is mainly used for enzymes. A simple system that was employed in early biosensors is the retention of enzymes on transducers, such as electrodes, by semi-permeable membranes, such as dialysis membranes [5]. Substrates and products can cross this barrier, but the enzyme cannot.

Biomolecules can also be confined in microcapsules of either semi-permeable materials or liposomes. However, even when the enzymes are immobilised in the microcapsules, association with the transducer is often difficult [5].

The more important advantages of the method are:

- the narrow contact between the enzyme and the transducer,
- it is easily applicable and
- there is stability in changes of pH, temperature and ionic force.

1.2.4.2 Chemical methods

1.2.4.2.1 Covalent Binding

The immobilisation of biomolecules on solid supports by covalent coupling usually leads to stable linkages. Proteins can be bound to an activated surface *via* their amino acid residues or terminal groups. These groups include amino, thiol, carboxyl, phenolic, imidazole, disulfide, hydroxyl and thioether groups [5].

An important factor for covalent immobilisation is the support material and especially the presence of functional groups. These functional groups can be present either directly at the solid support or be introduced *via* another matrix, such as membranes.

If an additional matrix is used to introduce functional groups to the solid support, the range of these groups is very broad. The reaction between membrane and protein sometimes involves chemical activation and mild chemistry, but often it is only required to dip the pre-activated membrane into a protein solution or apply a drop of this solution onto the membrane [5]. The variety and availability of these immobilisation procedures allow the comparison of different membranes for proteins. Every protein is different and has different amino acid residues exposed. Membranes exhibiting excellent results with one protein may be unsuitable for another. In other cases of covalent immobilisation, the solid support can be directly modified, resulting in a covalent bond between the support material and biomolecule [5].

2. Lipid membrane biosensors

2.1 Implementation of natural chemoreception

A membrane is a mosaic of different proteins embedded and dispersed in the phospholipid bilayer. These proteins may either attach to cytoskeleton or float freely in lipid bilayer. They define functional characteristics such as membrane transport, cell adhesion, intercellular communication, etc. Membrane proteins can act as

enzymes, channels, adhesion molecules [15]. Proteins exhibit many interesting biological and pharmacological activities.

Most cell membranes are composed of approximately 50% w/w lipids and 50% w/w proteins [15]. Lipids are amphiphilic structures, which consist of a polar head group and an attached hydrophobic hydrocarbon chain (*Figure 2.1*) [15]. The cis-trans isomeration due to the bending of the second alkyl chains renders the membrane flexible (as it is responsible for the molecular packing and fluidity) and, further, permits the transportation of small polar molecules across the bilayer body (as it provides the binding places for the molecules, thereby facilitating the 'hopping' across to the other side).

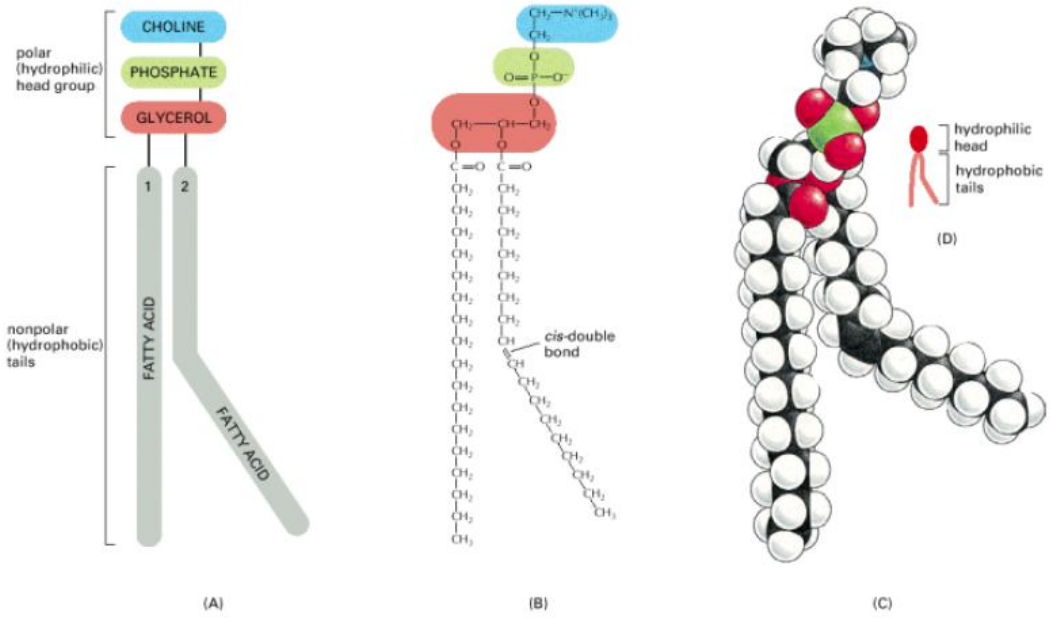

Figure 2.1: *The chemical structure of membrane phospholipids [15].*

There are two important regions of a lipid that provide the structure of the lipid bilayer: the hydrophilic and the hydrophobic region. The hydrophilic region is oriented towards the aqueous phase while the hydrophobic region is oriented towards the core. Due to their specific structure, phospholipids are allowed to form lipid bilayer membrane (BLM) and other configurations such as multilayers, micelles and liposomes. Micelles are relatively small, spherical structures composed of an aggregate of surfactant molecules dispersed in a liquid colloid. They can form when the lipid amount is low relative to water ratio and at the regions of membrane

instability. Liposomes are bilayered lipid vesicles formed by hydrating lipids in aqueous solution. Lipid molecules in lipid bilayers can change their conformation, rotate around their molecular axis, diffuse laterally, protrude out of bilayer plane, and flip-flop between the two monolayers [15]. This allows the membranes to be flexible, which is a property required for various modes of their principle functions.

Artificial lipid membranes are useful models to gain insight into the processes occurring at the cell membrane, such as molecular recognition, signal transduction, ion transport across the membrane [15]. These membranes are often used to characterize membrane proteins or to study membrane active systems, such as ion pumps or neural portals. Various methods have been used to create artificial lipid membranes including mainly free suspended membranes (i.e., membranes separating two aqueous phases) or membranes on solid supports (*Figure 2.2*) [15].

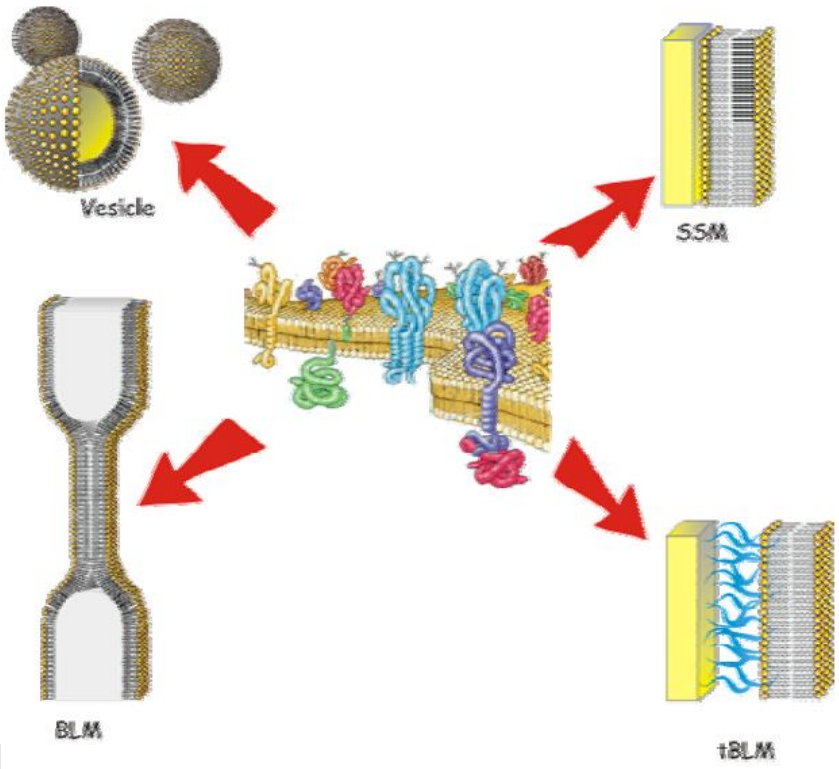

Figure 2.2: *Model systems used in biomimicing of cell membrane [15]: vesicles are formed on aqueous solution, usually by sonication; bilayer lipid membranes (BLMs) are formed between two aqueous phases, hold together by van der Waals forces (left) or attached on solid supports (right) directly (top right) or via glutaraldehyde cross-linking (bottom right).*

2.1.1 Conventional BLMs (c-BLMs)

Since the pioneering work on bilayer (black) lipid membranes (BLMs) in the early 1960s, several generations of membrane biophysicists and bioscientists have exploited the conventional BLM system for biophysical and reconstitution studies. Experimentally, a BLM is formed by painting a lipid solution. To date, the original method is still one of the simplest techniques available. A.L Ottova and H. Ti Tien [16] typically use for the construction of BLMs either a 1% phosphatidylcholine (lecithin) in n-decane or glycerol dioleate in squalene. A conventional BLM can also be formed by the Langmuir-Blodgett (LB) technique described in section 2.1.2. It should be mentioned, however, that there is a major difference between the BLM and multilayers formed by the LB technique. A BLM, formed either by the conventional 'painting' method or self-assembled on a substrate is a dynamic liquid-like structure which is capable of accommodating a host of modifiers [16]. In contrast, a Langmuir-Blodgett multilayer of bimolecular thickness, albeit much more stable than a BLM, usually contains pinholes and is in a solid state. In this connection efforts to stabilize BLMs by using polymerizable lipids have been successful. However, the electrochemical properties of these BLMs were greatly compromised. A conventional BLM can, also, be formed in a horizontal way, which was initially used to 'blow' a single, spherical BLM or a giant liposome [16]. The so-called 'solvent-free' BLMs, is a misnomer at best.

Proteins including ion-channel formers may be reconstituted into BLMs by incorporating the proteins first in a liposome then by fusing it with the BLM, which takes place readily [16]. In a sense, the lipid bilayer as existing in BLMs and liposomes may be considered as a solvent for a number of hydrophobic materials including proteins. In this connection it should be mentioned that unmodified or pure liposomes can also induce channel-like activities in BLMs [17].

To modify the intrinsic properties of BLMs (modified BLMs), many classes of compounds have been embedded, including [16]:

- electron acceptors, donors, and mediators, highly conjugated compounds such as meso-tetraphenylporphyrins (TPP), metallo-phthalocyanine (PLC), TCNQ (tetracyano-p- quinodimethane), TTF (tetrathiafulvalene), BEDT-TTF (bis-ethyl-dithio-tetrathiafulvalene), tetraseleno-fulvalene and fullerenes (C60, C70),

– Redox proteins and metalloproteins such as cytochrome c, and iron-sulphur proteins (ferrodoxins and thioredoxins). Also included in this class are compounds partaking in ligand-receptor contact interactions. Specifically, the ligand may be a substrate, an antigen, a hormone, an ion, or an electron acceptor or donor, and the corresponding receptor embedded in the BLM may be an enzyme, an antibody, a protein complex, a carrier, a channel, or a redox species, and fine semiconductor particles (formed in situ) such as CdS, CdSe, and AgCI.

Modified BLMs will be further analysed in *Section 2.2.2*.

2.1.2 Langmuir-Blodgett (LB) films

It has long been known that organic materials can spread upon a water surface to form a thin film. Most of the molecules which form these layers are amphiphilic [18]. Gaines in his 1966 book widely reviewed many of these insoluble monolayers [18]. Much early work on the structure of these monolayers was performed by Langmuir [19], who later in collaboration with Katharine Blodgett first described the transfer of these monolayers onto a solid substrate. Blodgett later published details of extensive research into deposition of fatty acids and postulated they had a well-ordered layer structure [20].

In essence, Blodgett dissolved amphiphilic molecules in a water-immiscible organic solvent which was carefully cast onto a clean water surface [20]. The solvent evaporates leaving behind a disordered layer of the amphiphiles. Barriers are then moved across the surface, compressing the layer and causing the molecules to pack more closely (*Figure 2.3*) [18]. Finally a quasi-two-dimensional solid is obtained where the molecules are closely packed and all aligned in the same direction with their hydrophilic headgroups on the water surface [18].

This monolayer can often be compressed to quite a high surface pressure until eventually over-compression of the layer beyond this point causes collapse to a multilayer structure.

If a clean substrate is passed through a suitable compressed monolayer into the water subphase, a monolayer of the amphiphile attaches to the substrate, when withdrawn a second layer can attach as shown (*Figure 2.4*) [18]. If the surface

pressure is maintained this process can be repeated to build-up multilayers of any required thickness.

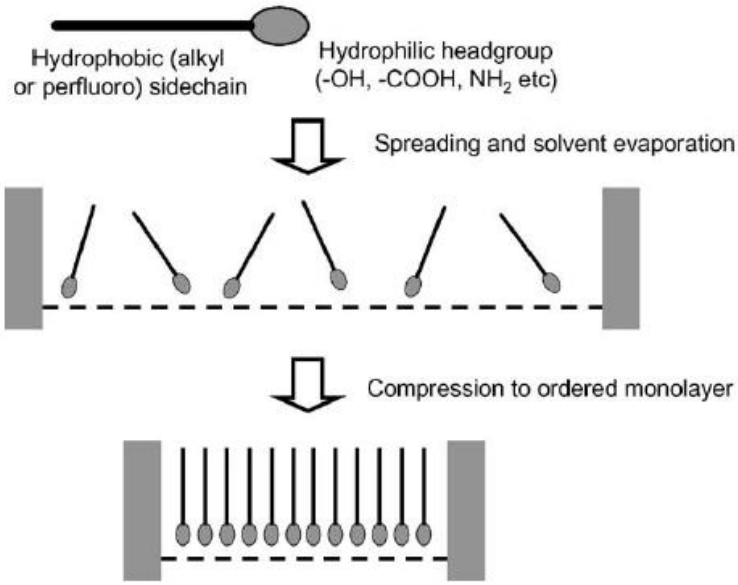

Figure 2.3: *Formation of an ordered monolayer at the air-water interface, adapted from [18].*

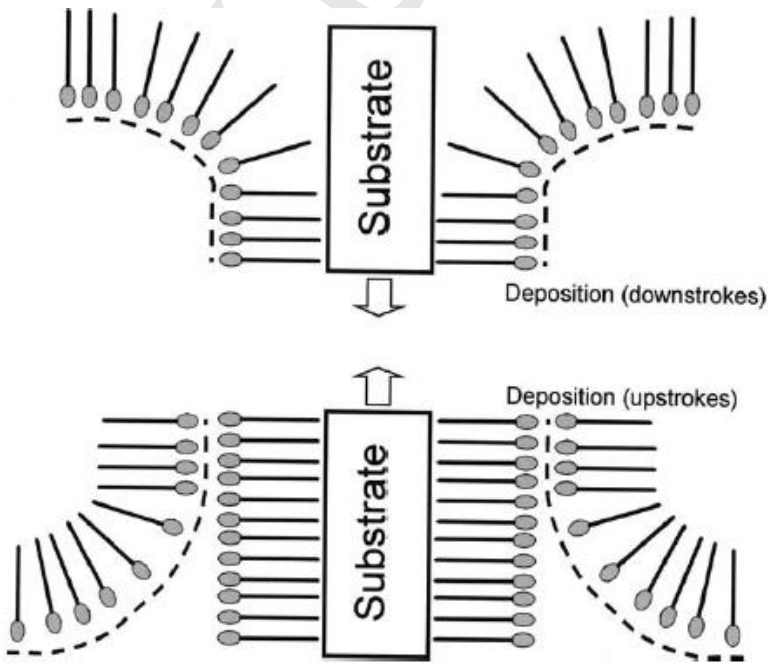

Figure 2.4: *Deposition of a Langmuir-Blodgett multilayer, adapted from [18].*

2.1.3 Structural aspects of BLMs

The monolayer is a thermodynamically unstable structure existing only in the gaseous or liquid state or on solid substrate not in aqueous media. On the other hand the BLM is metastable and can be viewed as the limiting unit of the mesomorphic or smectic (neat) liquid-crystalline phase [21]. The formation of BLMs is a spontaneous self-assembling process, the thermodynamics and the stability of which have been analyzed in terms of the, hydrophobic and repulsive contributions [21]. It should be noted that phospholipid BLMs are capable of undergoing a variety of lyotropic and thermotropic phase transitions, which are affected by the composition of the aqueous phase. In general, at low temperature, ($< 30^{o}C$) the BLM structure corresponds to a lamellar crystalline state. At higher temperatures, the steric and Van der Waals interactions are counteracted by the thermal agitations. The BLM undergoes transitions, first, to a lamellar gel phase, then to a "fluid" bilayer phase [21]. Experimental evidence suggests that the BLM chain "melting" takes place as follows [21]: first, an alkyl chain undergoes cis-trans isomerisation, which happens at random and is the nucleation step for transition. The process causes distortion in chain orientation which migrates from chain to chain and creates density fluctuation [21]. This follows by the relaxation of the density regions via lateral expansion with increasing lipid mobility in the lipid bilayer interior and at the polar-hydrocarbon interface, which results finally in the fluid bilayer phase [21].

2.1.4 Transmembrane ion transport in BLMs

To transport a solute or solvent molecules across a membrane such as a BLM, a driving force must be present, i.e. a gradient of chemical potential, electrochemical potential, electrical potential, pressure, or temperature. The pathway across the BLM may be facilitated by carriers or channels. To describe membrane transport, three approaches have been used [21]:

- the Nernst-Planck equation.
- the absolute reaction rate theory, and
- the nonequilibrium thermodynamics

Experimental evidence indicates that the resistance to solute permeation is most likely located in the interfacial region, although the membrane phase (lipid bilayer core) can also be the rate-limiting barrier. As expected, the rate of material transport,

across BLMs increases with increasing temperature, being particularly so at the phase transition temperature. However, other factors such as ion-binding and lipid flip-flop rate at increased temperature may be also important.

2.1.5 Experimental aspects of BLMs

Movements of charged species (ions, electrons, holes) across a BLM constitute electric currents. Electrical parameters that have been measured on BLMs are membrane potential (E_m), resistance (R_m), current (I_m), capacitance (C_m), breakdown voltage (V_b) and I/V curves (voltammograms) [21].

According to A.L Ottova and H. Ti Tien the usual electrical parameters are [16]:

- capacitance (C_m) about 1μF cm^{-2}
- resistance (R_m) greater than 10^8 ohm cm^2 and
- breakdown voltage or dielectric breakdown (V_b) at about 300000 V cm^{-1} and
- very low interfacial free energy about 0.5 erg cm^{-2}.

2.2 Electrochemistry of membranes

2.2.1 Mechanism of signal generation

A. Ottova-Leitmannova and H.T. Tien and others have shown experimentally with modified BLM that the membrane, in addition to serving as a physical barrier separating two compartments, acts as a bipolar electrode, that is, there is an anodic oxidation on one side of the membrane and a cathodic reduction on the other side, with the membrane itself (lipid bilayer) providing pathways for electrons and protons, forming this way ion channels that allow the rapid and selective flow of inorganic ions across the lipid bilayer of biomembranes [21, 22]. These ion channels generate electrical signals.

2.2.2 BLMs Modifiers

Over the years, techniques have been developed to incorporate a wide variety of compounds into BLMs to endow them with desired properties. These incorporated membrane active compounds can be divided into six categories, namely, those [23]:

- altering the ionic electrical properties,
- conferring ion specificity,
- inducing electrical excitability,
- changing the mechanical properties,
- generating photoelectrical effects, and
- imparting electronic characteristics.

2.3 Self-Assembling Bilayer Lipid Membranes on Solid Support (s-BLMs)

The fragility of the free-suspended BLMs has prompted research towards more stabilised structures. The incorporation of cholesterol, or the support of free-suspensions on nylon fibres or other support material (thiol bridges, gold supports, etc.) resulted in rigid structures that exhibited, however, decreased sensitivity since the molecular packing and fluidity of the bilayers was significantly decreased, rendering them unsuitable for enzyme- or receptor based biorecognition. Ottova-Leitmannova and Tien described a simple mechanical procedure for the self-assembly of lipid bilayers on solid supports (*Figure 2.5*) [23].

The s-BLM is typically formed on the tip of a solid support. The formation of an s-BLM is accomplished in two basic steps [22]. In the first step, the tip of a freshly cut metal wire is immersed in a lipid droplet. The wire is usually coated with some type of insulator. The rough freshly cut surface has many pits and crevices in it, which makes it difficult for the polar heads of the lipid molecules to bind to the support. However, the 'fluid' and dynamic nature of the lipid bilayer alleviates this problem [22]. In the second step, the tip of the freshly cut metal wire with the lipid droplet is submerged in an aqueous solution. After a few minutes, a stable lipid bilayer will be formed on the tip of the wire. Electrical properties are utilized to follow the thinning process of the BLM formation [22]. When the increasing slope of the capacitance and the decreasing slope of the resistance begin to level off, this indicates the presence of a self-assembled planar lipid bilayer (s-BLM) [22]. The hydrocarbon interior of the bilayer membrane is responsible for these electrical properties (e.g., R_m and C_m).

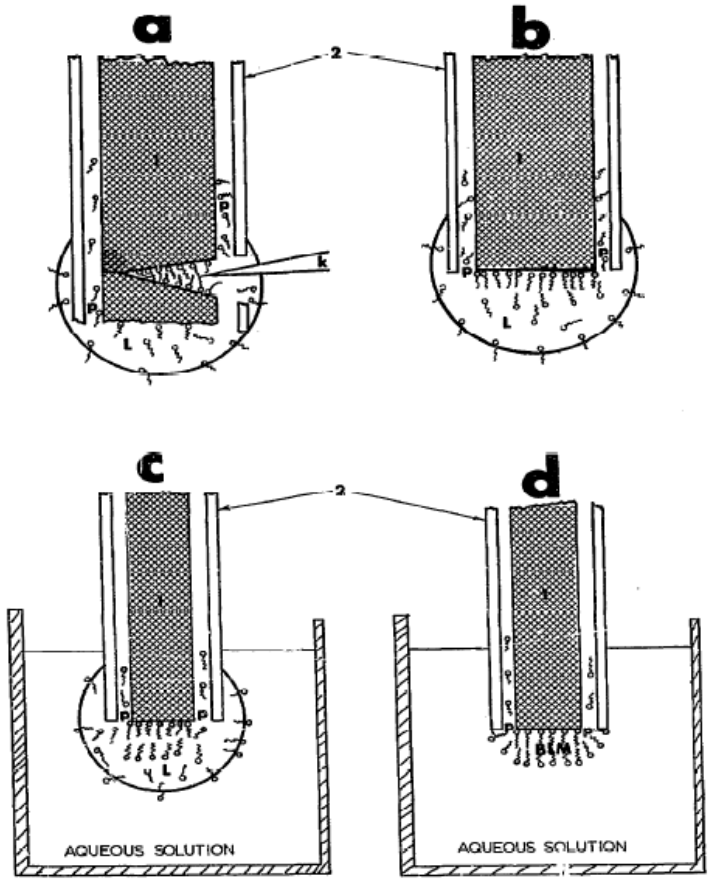

Figure 2.5: *Diagrammatic representation of the self-assembly process: (a) the freshly cut tip of the electrode is dipped into the lipid solution and then it is transferred into the working cell; (b) within the lipid phase, the lipid starts forming a micelle-type formation around the electrode tip, with a number of lipid molecules are oriented towards the groovy metal surface (polar heads attached to the metal, tails facing the inside of the micelle); (c) within the aqueous phase, the micelle starts to collapse due to the electrostatic interactions, directing the lipid molecules towards the metal-attached monolayer. (d) after some time (10-40 minutes) any multi-layer formation is broken down, leaving a clear bilayer insulating the tip of the electrode immersed in the water.*

These supported lipid bilayers retain a high degree of their flexibility and have a long life, thereby offering opportunities for the preparation of a variety of probes with diverse applications in membrane biophysics, biochemistry, physiology and in biotechnology. Supported bilayer lipid membranes (s-BLMs) have been employed for embedding a variety of compounds such as peptides, enzymes, antibodies, receptors, ionophores, and redox species in detecting their respective counterparts, such as

substrates, antigens, hormones, ions, and electron donors or acceptors (*Figure 2.6*) [21].

It is important to note that the BLMs formed here is liquid-crystalline in structure that enables it to be modified for basic studies. The construction of the s-BLM made it very easy to be tested for many electrical parameters. For example, as already having an electrical contact on one side of the membrane, essentially all that is needed to test for the potential difference across the BLM is to have a reference electrode (e.g., Ag/AgCl) in the bathing solution. Unlike c-BLMs, the structural state of s-BLMs and, therefore, many of the mechanical and electrical parameters can be modified by applying a dc voltage. Furthermore, an s-BLM formed in the manner described above is remarkably stable; simple washing or mechanical agitation cannot remove it.

However, an s-BLM may be detached from its metallic substrate by sonication, electrochemically or by drastic chemical treatments. Although usually depicted lipids are oriented perpendicular to the metal surface, however, they are most likely tilted in some angle from the normal [22]. To cover any surface by a layer of lipid molecules at the molecular dimension is an extremely difficult task, since the morphology of the substrate is not likely to be 'smooth'. As an experimental fact, monolayers and multilayers of lipids prepared by the LB technique, described in *Section 2.1.2*, are often full of pinholes. These defects are hard to avoid owing to the nature of the substrate at the atomic level [22]. Thus, a freshly cleaved metal surface is not smooth at the atomic level; it is most likely to be very rough with grain and edge boundaries. However, the lipid solution used, being a fluid, is able to interact with the 'bumpy' terrain of the newly cut metal surface and to form an intimate attachment within its indentations, pits, and crevices [22]. The lipid monolayer adjacent to the solid metal support is presumed to be stabilized by hydrogen bonds arising between the hydrophilic groups of the monolayer and the electronegative metal surface [22]. The hydrophobic alkyl tails of the amphipathic lipid molecules are arranged in such a way, which allows the polar head groups to pack more closely [22]. The final self-assembling lipid bilayer is stabilized because of intermolecular forces. The breakdown voltage of s-BLMs under these conditions is several times higher than conventional BLMs (up to 1.5 V or more) [22]. The most important factor in the process of the s-BLM preparation seems to be the time the cut end of the wire is allowed to remain in the membrane forming solution prior to its transfer into the aqueous solution for a supported BLM to self-assemble.

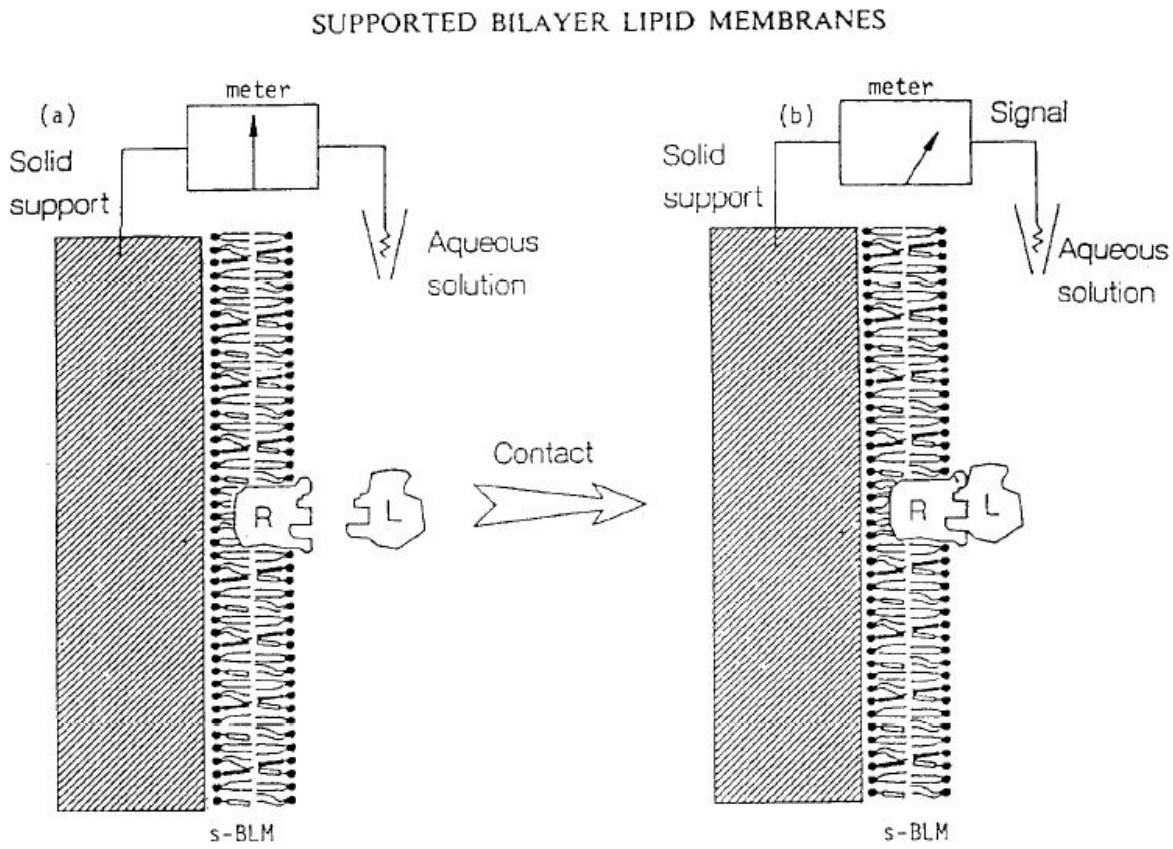

Figure 2.6: *Supported BLMs (s-BLMs) based electrochemical/biosensors. The essential idea is that ligand (L) and receptor (R) contact interactions are the principal mechanisms underlying almost all physiological activities [21].*

2.3.1 Ellipsometric determination of(s-BLMs) on silver metal

The stability and reproducibility of these s-BLMs for applications as biosensors suggests that these systems may be suitable for the development of practical devices. However, fundamental questions remain about the actual structure, and therefore the confidence and reliability, of s-BLMs. Many researchers investigated the self-assembly process, and especially whether lipid membranes spontaneously thin to form ordered lipid assemblies of bilayer dimensions on surfaces such as silver metal. Electrochemical studies alone provide only indirect evidence which supports the concept of formation of a modified BLM [25]. Ellipsometry (performed through aqueous electrolyte solution) of lipid films on silver metal surfaces has now allowed direct measurement of the thickness of the lipid films. It seems that the films spontaneously thin to achieve monolayer, bilayer or trilayer dimensions, and suggest

that caution in presumption of BLM thickness should be present when fabricating sBLMs on metal wire platforms [26]. It should be noted, however, that values which are determined by ellipsometric measurements are relative thickness values which were obtained by comparison of thickness values for bare substrates and substrates which were covered with an immobilized membrane.

For silver metal pads, the time dependence of the thinning process was related to whether the lipid was first dried, and then placed in aqueous solution (*Diagram 2.1*), or whether the lipid solution was covered with aqueous solution (*Diagram 2.2*). The time for hydration and thinning of a dried lipid film took about 30 min, while a lipid solution could thin to bilayer dimensions in a period of 15 to 20 min [25].

The absolute thickness values are made less reliable owing to the fact that the immobilized membrane system is not ideal for ellipsometry in that it violates several assumptions of the Drude equations. Kuang-Lee Chiang et al. [25] proposed that:

- the film is likely oriented with alkyl chains perpendicular to the water-film boundary and is therefore uniaxially anisotropic,
- it is possible that the surfaces are not smooth and that the boundaries between ambient, film and substrate are not plane parallel,
- it is possible that the films are discontinuous and present in the form of patchy overlayers.

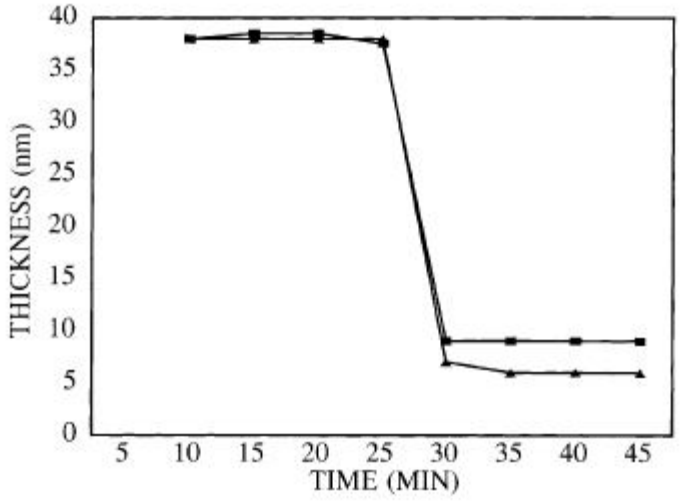

Diagram 2.1: *Time course of thickness changes observed for dried lipid films on silver metal pads that where deposited directly onto PVDF.*
Diameter of metal pads: 5.5mm (■) *and 7.5 mm* (▲) *[25].*

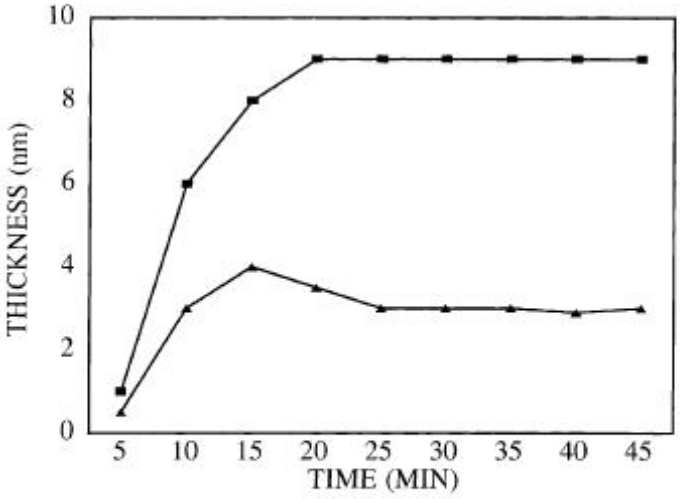

Diagram 2.2: *Time course of thickness changes observed for dried lipid solutions on silver metal pads that where deposited directly onto PVDF.*
Diameter of metal pads: 3.5mm (■) *and 5.5 mm* (▲) *[25].*

A useful indication of the reliability of the ellipsometric measurements can be obtained by the study of a lipid film sample of known thickness and coverage. Such a sample can be prepared by the deposition of a monolayer of lipid that has been prepared at an air-water interface, onto a substrate by the technique of Langmuir-Blodgett film casting. The results indicated that the monolayers had an average thickness of 3.0±1.6 nm, which is consistent with the absolute value of thickness expected for such a lipid film [25].

Clearly the effects of surface tension and adhesion of the lipids to the silver pads will not be identical to that encountered in the previous electrochemical experiments using wire electrodes of different diameters. While most work with s-BLMs makes use of metal wires of diameter of 1 mm or less, it was not possible to use analogous metal pads of such small diameter in the ellipsometry experiment. The source spot size and angle of reflection used during ellipsometry limited the diameter of the silver pads to values greater than 3 mm so that the laser spot only sampled reflective metal [25].

3. Biosensors for the control of environmental parameters

3.1 Scope and objectives of the work

The scope of this work is the design of environmental biosensors taking into consideration environmental constraints, needs, and parameters that will allow informed decisions to be made regarding the ecosystem status. Two approaches were followed in this project: a knowledge-based approach and an analytical development approach.

At first, the knowledge-based approach allows the design of a methodological framework for the monitoring of the ecosystem status. In this work we used as an example for the development of the methodology the monitoring of polycyclic aromatic hydrocarbons (PAHs) in estuarine areas. In this context, the analytical development approach involves the construction of biosensor device, using self-assembled bilayer lipid membranes, supported on the electrode surface. As a case example, a horseradish peroxidase (HRP) biosensor was constructed, validated against commercial hyperoxide solutions.

3.2 Methodological Framework

The methodological framework, designed to support biosensor development custom-tailored to environmental needs, processes and resources (*Figure 3.1*), follows a knowledge-based approach aiming at ensuring that a site-specific assessment tool will be suitably constructed to provide information on critical ecosystem parameters that will allow informed decisions to be made regarding the ecosystem status. In the environment, multiple species of microorganisms share one ecological niche (e.g. degradation of a given pollutant); among these, one population (or a few) that best adapts to the ecosystem conditions becomes predominant, while others exist as minorities. These species assume the burden of managing the given pollutant, i.e., their cellular degradation mechanism is more sensitive, selective and robust than that of other species that use their resources for survival purposes only. The predominant

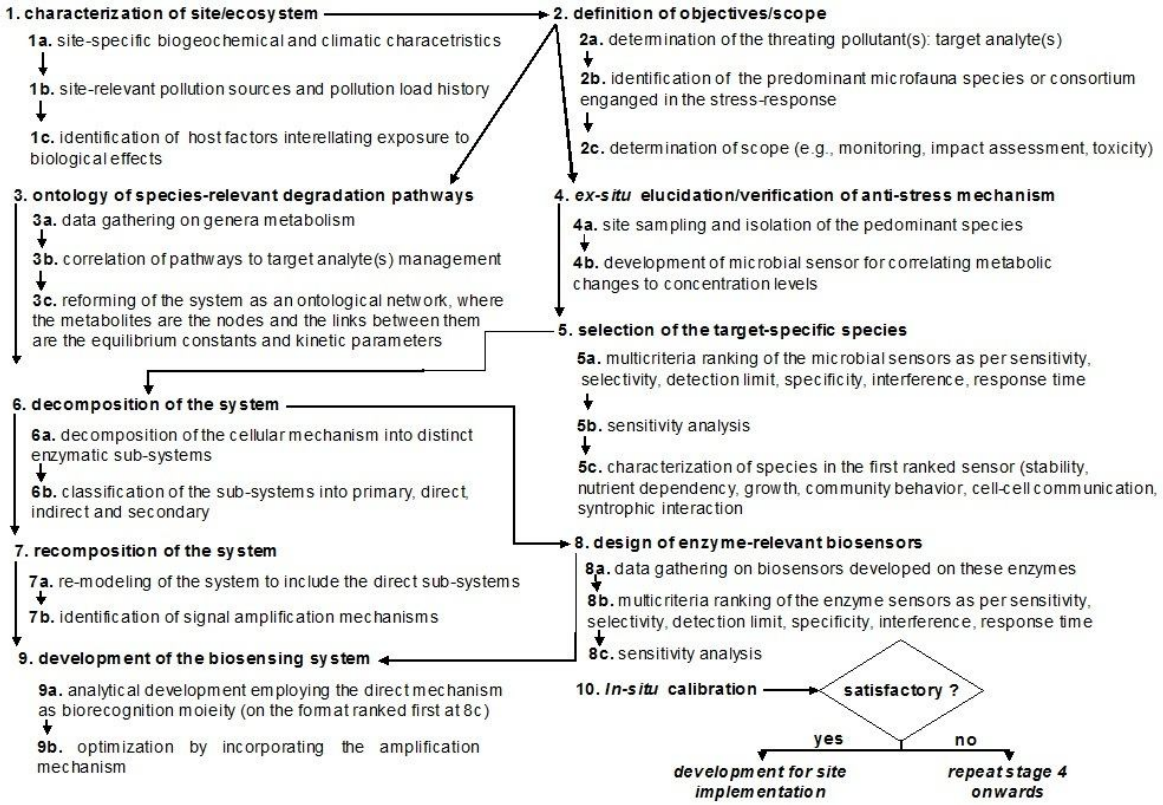

Figure 3.1: *Overview of the methodological framework designed to support biosensor development custom-tailored to environmental needs, processes and resources. All the steps of the framework are effectuated through a Knowledge Base (KB) developed on the ontological platform reported in [2] to suit the needs of the proposed scheme.*

species, when used as biorecognition elements in microbial biosensing set-ups, can be easily identified (step 5) on the basis of the analytical characteristics of the sensors.

Thereafter, the whole-cell is considered as a pollution impact simulator, assuming simultaneously an active role in toxicant degradation and a passive role as impact recipient. This simulator can be decomposed into functional sub-systems (step 6), elucidating the parts of the cellular mechanism that weigh most on pollution management (step 7). Thereby, site-derived and target-specific biosensor systems can be developed (step 9) for the reliable assessment and monitoring of the ecosystem status. The proposed scheme is easily adopted to biomonitoring or bioremediation projects, as it can be used to (i) identify representative species, (ii) explicate and/or relate visual damage to systemic adjustments/changes, (iii) optimize biotic parameters, and (iv) validate/characterize genetically engineered species.

3.3 Implementation

3.3.1 Field biosensors for monitoring polycyclic aromatic hydrocarbons (PAHs) in estuarine areas-A knowledge-based approach

The methodological framework described above has been implemented in the development of field sensors for polycyclic aromatic hydrocarbons (PAHs) in estuarine areas. Due to their hydrophobic nature, most PAHs are associated with sediments where they may become buried and persist until degraded, resuspended, bioaccumulated or removed by dredging [27]. Toxicological data for some of the lower-molecular-weight aromatic hydrocarbons, such as naphthalene and its methylated derivatives, puts them on top of the priority concern list. Although much is known on the metabolism and bioactivation or detoxification of PAHs by pure cultures in the laboratory, much less is known about the rate and chemical pathways in water/sediment interfaces.

The degradation of naphthalene in the environment can be affected by several factors which may differ among ecosystems (or even within the same ecosystem) [28, 29], such as organic and inorganic nutrient levels, temperature, pH, salinity, previous chemical exposure, microbial adaptations, and oxygen tension (step 1c). Many species of bacteria and fungi may be involved in the degradation process, acting independently or synergistically.

A large number of species on various community structures has been retrieved by the KB as naphthalene catabolizers in sediment/water interfaces. The acting communities have been limited down to four consortia (step 2b), in which γ-Proteobacteria (namely *Pseudomonas* spp.) can be considered as the predominant consortium in the ecosystem under investigation (*Figure 3.2*). This species is commonly used in biosensors [30], and the relevant literature on analytical characteristics is rich; yet the degradation mechanism *per se* has not been fully elucidated. After constructing the ontological network of the possible metabolic pathways (3c), thinning (as described in [31] for biological processes) yielded the deoxygenase-based breakdown process (*Figure 3.3*) as the most possible mechanism under the conditions studied (step 7a). Six sub-systems have been identified as suitable candidates for step 9a, serving detection, pathway verification and metabolites screening. Enzymic reactions 1, 3 and 5/6 can be used for quantifying naphthalene; similar biosensing formats have been reported for the first two enzymes,

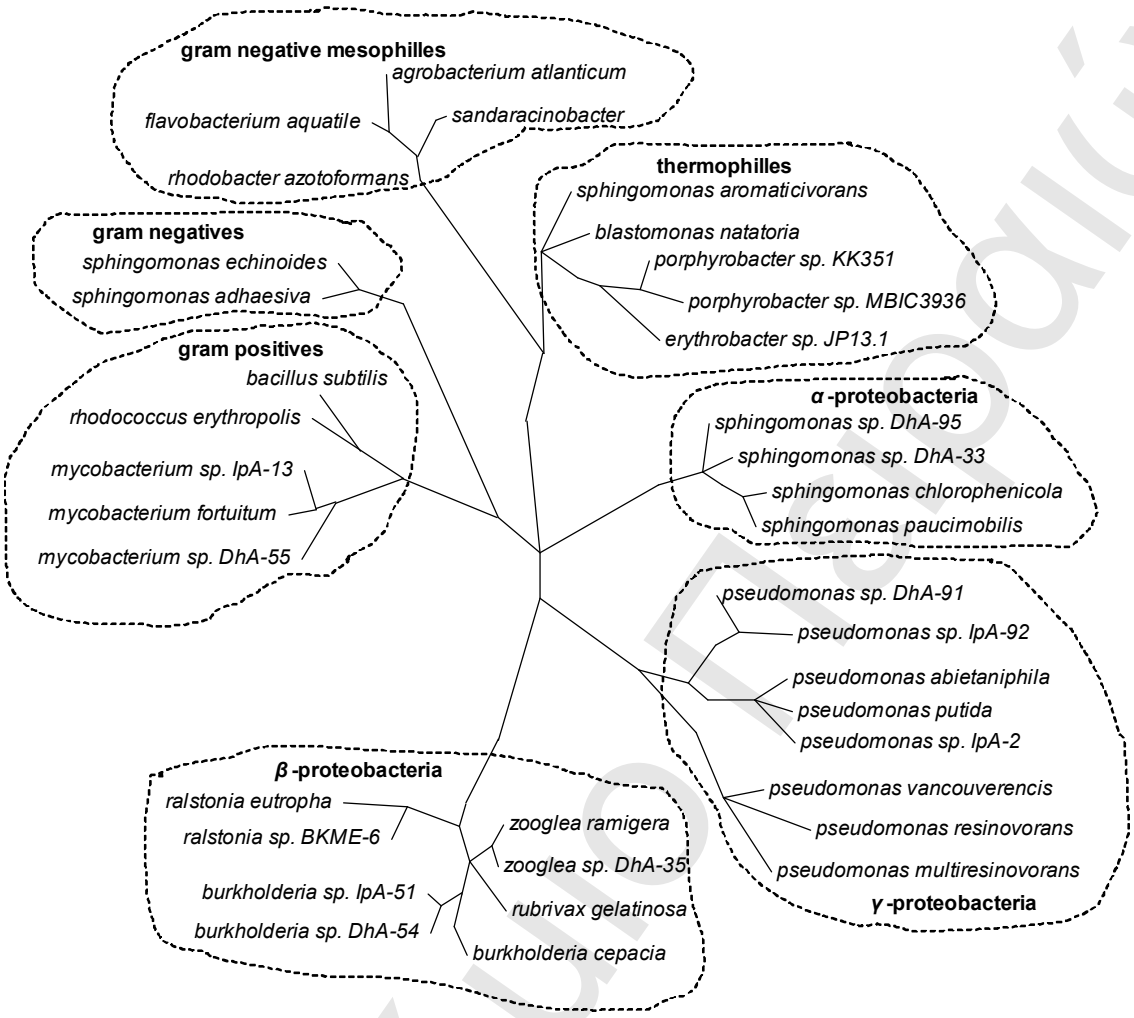

Figure 3.2: *An unrooted phylogenetic tree for naphthalene degraders in sediment/water interfaces. The synergistic communities of interacting species.*

namely naphthalene-1,2-deoxygenase and 1,2-dehydroxynaphthalene deoxygenase, commonly shared among *pseudomonas* genera.

The hydratase-aldolase-catalyzed conversion of trans-o-hydroxybenzylidene pyruvate to salicylaldehyde and pyruvate is an intermediate reaction in the conversion of naphthalene to salicylate. As it was found out in [29], the presence of naphthalene inhibits the reaction, making possible the development of an indirect biosensor, where the decrease of pyruvate concentration could be related to naphthalene concentration in samples. The subsequent reaction involving salicylaldehyde dehydrogenase serves *in vivo* as signal amplifier (step 7b) and should be included in the biosensor format. The catabolism of catechol produced during the metabolism of naphthalene by *pseudomonas* spp. has previously been shown to involve the meta (or a-ketoacid) pathway [27], although the ortho-path has been also reported [28]. Pathway selection

and/or predominance has been correlated to plasmid regulators and assumed to be controlled genetically as a unit. However, recent studies suggest that although the pathways may be readily interchanged *in vivo*, their regulation is not genetically controlled making plasmid extrapolation for molecular engineering largely ineffective. The clarification of the pathway followed, utilizing the enzymes 9, 18 and 24/25, and the study of the conditions under which each path is activated, is vital to ecotoxicology engineering.

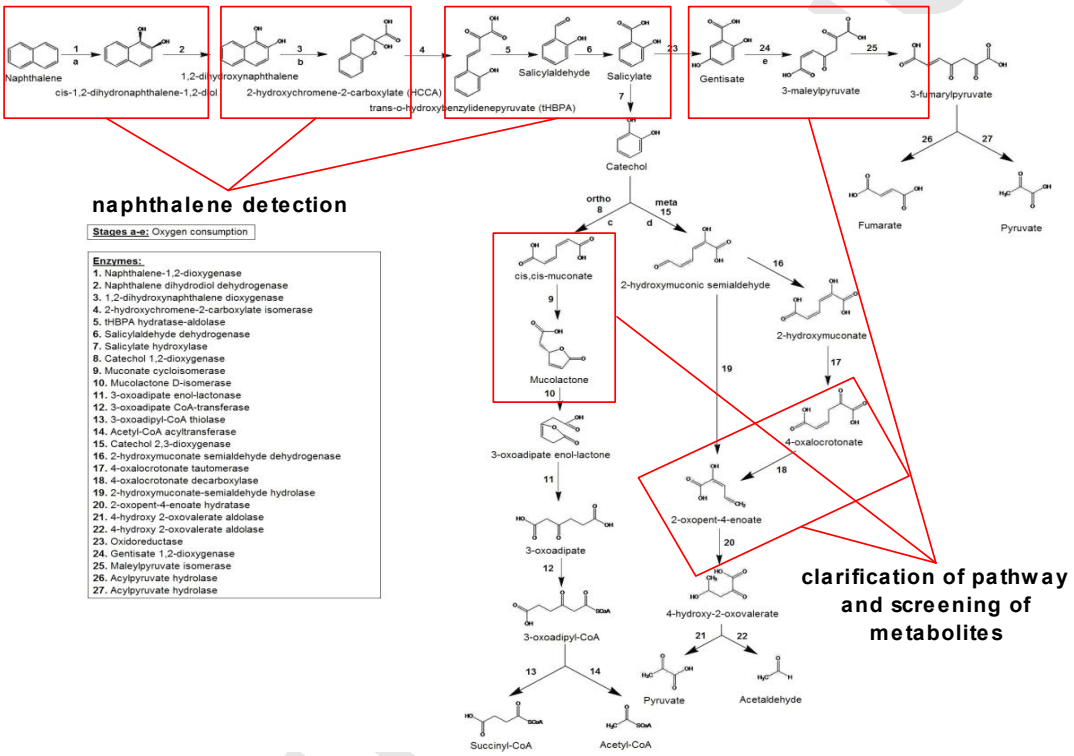

Figure 3.3: *Primary pathway of naphthalene biodegradation in Pseudomonas spp. (as retrieved at step 7a of the methodological framework presented in Figure 3.1). The biodegradation of naphthalene has several stages which are performed mainly by oxygenases and feature consumption of oxygen resulting in the breakdown of the aromatic rings. Naphthalene deoxygenase activates cell respiration, justifying the suitability of the species for microbial sensor development. All the reactions shown involve electron transfer, thus enabling the utilization of the enzyme sub-systems in amperometric biosensing. Six such sub-systems (boxed) have been identified as suitable for step 9a, relating to naphthalene detection, pathway verification and metabolites screening.*

3.3.1.1 Commentary on results

The proposed scheme, exploiting site-derived anti-stress response mechanisms as a molecular tool for developing site-specific field measuring systems, integrates effectively multiple layers of knowledge in order to link abiotic parameters to ecological quality and provide the necessary information granularity in a single assessment framework. Thereby, the developed biosensors assess the ecological effects of pollution rather than pollution itself, guiding advances on ecotoxicology, ecological microbiology, bioremediation and biomonitoring.

3.3.2 Construction of Horseradish (HRP) biosensor for hyperoxide detection - Analytical development

Implementing stages 8 and 9 of the methodological framework, this work involves, as a case example, the construction of an HRP amperometric biosensor for the detection of commercial-grade H_2O_2. Since HRP is capable of reducing H_2O_2 and also some organic peroxides, HRP-based biosensors are widely used to detect these peroxides for environmental biomonitoring. Several HRP based biosensors for the detection of small molecules other than H_2O_2 have been developed in recent years, which include peroxides such as, *t*-butyl hydroperoxide, 2-butanone peroxide, cumene hydroperoxide, etc. (see [32] and references stated therein); HRP-based biosensors are also the most sensitive for a great number of compounds that act as electron donors, such as phenolic compounds.

In bioelectrochemistry, peroxidase studies have been numerous, and since the late eighties considerable interest has been paid to the development and characterization of HRP-modified electrodes [33-35]. Such electrodes allow both direct and mediated electron transfer reactions for substrates, inhibitors and activators of the enzyme. The interest in HRP is derived from the possibility of direct electron transfer between the enzyme and the electrode matrix, allowing the construction of reagentless electrochemical biosensors [36].

The mechanism for the detection of such compounds is described bellow: enzyme molecules are re-reduced by phenolic compounds after they are oxidized by hydrogen peroxide on the surface of the electrode (*Figure 3.4*) [37].

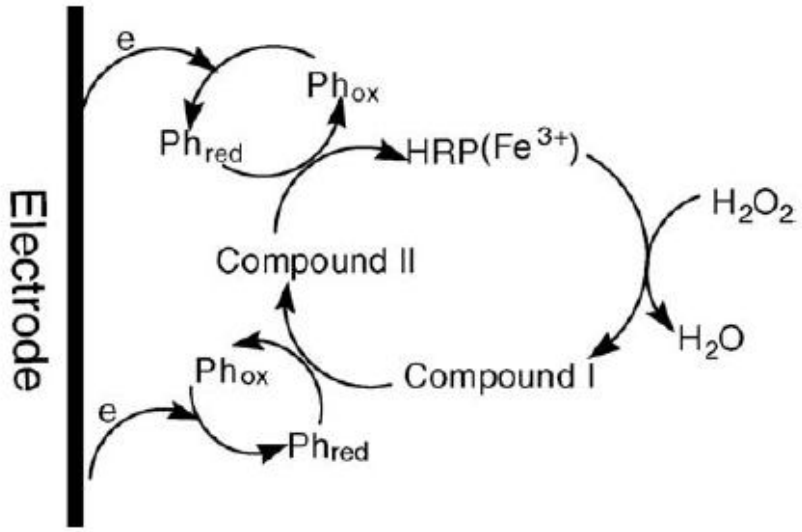

Figure 3.4: *Scheme of the reactions occurring at the surface of the HRP modified electrode for the determination of phenolic compounds.* Ph_{ox} *and* Ph_{red} *are the oxidized and the reduced forms of the phenolic compounds, respectively [37].*

3.3.2.1 Horseradish Peroxidase

Peroxidases, in general, catalyze oxidation of a large variety of substrates by hydrogen peroxide. This reaction gives an efficient way for removal of toxic hydrogen peroxide from the intracellular region [38].

Plant peroxidases, e.g. horseradish peroxidase, and fungal peroxidases, e.g. yeast cytochrome *c* peroxidase, consist of about 300 amino acids and non-covalently bound heme, whereas mammalian peroxidases are much larger (576-738 amino acids) and heme is covalently bound [39]. On the basis of amino acid sequence homologies, three families of plant peroxidases have been proposed: class I, prokaryotic peroxidases, e.g. yeast cytochrome *c* peroxidase and plant ascorbate peroxidases (smallest peroxidase with 251 amino acids); class II, secretory fungal peroxidases; and class III, secretory plant peroxidases (ER-targeted), e.g. horseradish peroxidase isoenzyme C [39]. Class III peroxidases contain structural Ca^{2+}, disulfide bridges and are targeted for the secretory pathway via the endoplasmic reticulum [39].

Horseradish peroxidase is the most widely studied member of this peroxidase family. HRP is a monomeric heme-containing plant enzyme (44 kDa) which has found enormous diagnostic, biosensing, and biotechnological applications because of its unusually high stability in aqueous solution [38].

The crystal structure of HRP (*Figure 3.5*) has been solved recently. The structural features of HRP include two Ca^{2+} binding sites proximal and distal to the heme, four disulfide bridges (Cys11-Cys91, Cys44-Cys49, Cys97-Cys301, and Cys177-Cys209), N-glycosylation, and an extensive hydrogen- bonding network [38]. These may aid in stabilization of the secondary and/or tertiary structure of the enzyme. The iron of the heme prosthetic group of HRP was found to be penta-coordinated, the distal and proximal sites of the heme pocket were shown to have a hydrogen-bonding network, and the residues participating in this network were also identified in the enzyme from the crystal structure [38]. The three-dimensional structure will be discussed in detail in *Section 3.3.2.1.2.*

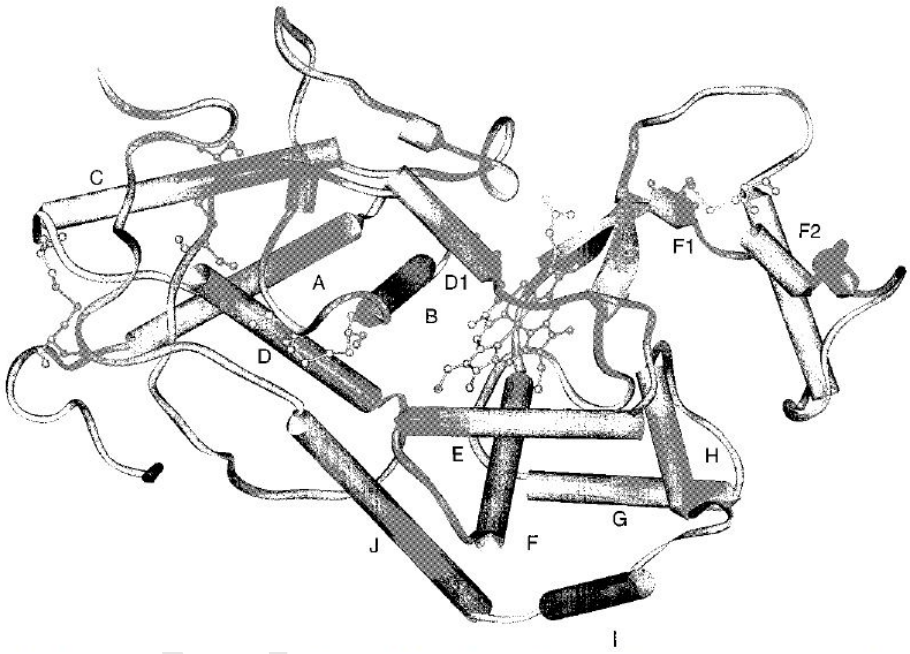

Figure 3.5: *Structure of HRP obtained from the crystallographic results [38].*

It is now accepted that peroxidases occur as a large family of isoenzymes. Isoenzymes (or isozymes) are different molecular forms of the same enzyme, which catalyse the same biochemical reaction but have distinct physical, chemical and kinetic properties arising from small differences in their amino acid sequence [40]. Before the development of chromatographic techniques, it was already known that multiple forms of HRP existed throughout the whole plant.

3.3.2.1.1 General features of HRP

Horseradish peroxidase isoenzyme C comprises a single polypeptide of 308 amino acid residues. The N-terminal residue is blocked by pyroglutamate and the C-terminus is heterogenous, with some molecules lacking the terminal residue, Ser308 [40]. There are 4 disulphide bridges between cysteine residues 11-91, 44-49, 97–301 and 177-209, and a buried salt bridge between Asp99 and Arg123 [40]. Nine potential N-glycosylation sites can be recognised in the primary sequence from the motif Asn- X-Ser/Thr (where 'X' represents an amino acid residue) and of these, eight are occupied [40]. A branched hepta-saccharide accounts for 75 to 80% of the glycans but the carbohydrate profile of HRP C is heterogeneous, and many minor glycans have also been characterised. These invariably contain two terminals GlcNAc and several mannose residues [40].

A further complication is the variation in the type of glycan present at any of the glycosylation sites. The total carbohydrate content of HRP C is somewhat dependent on the source of the enzyme and values of between 18 and 22% are typical.

HRP C contains two different types of metal centre, iron (III) protoporphyrin IX (usually referred to as the 'heme group') and two calcium atoms (*Figure 3.6*). Both are essential for the structural and functional integrity of the enzyme. The heme group is attached to the enzyme at His170 (the proximal histidine residue) by a coordinate bond between the histidine side-chain $N_{\epsilon}2$ atom and the heme iron atom [40]. The second axial coordination site (on the so-called distal side of the heme plane) is unoccupied in the resting state of the enzyme but available to hydrogen peroxide during enzyme turnover [40]. Small molecules such as carbon monoxide, cyanide, fluoride and azide bind to the heme iron atom at this distal site giving six-coordinate peroxidase complexes. Some bind only in their protonated forms, which are stabilized through hydrogen bonded interactions with the distal heme pocket amino acid side-chains of Arg38 (the distal arginine) and His42 (the distal histidine) [40].

The two calcium binding sites are located at positions distal and proximal to the heme plane and are linked to the heme-binding region by a network of hydrogen bonds. Each calcium site is seven-coordinate with oxygen- donor ligands provided by a combination of amino acid side-chain carboxylates (Asp), hydroxyl groups (Ser, Thr), backbone carbonyls and a structural water molecule (distal site only) [40]. Loss of calcium results in decreases to both enzyme activity and thermal stability and to subtle changes in the heme environment that can be detected spectroscopically.

3.3.2.1.2 HRP three-dimensional structure

The structure of the enzyme is largely α-helical although there is also a small region of β-sheet (*Figure 3.6*). There are two domains, the distal and proximal, between which the heme group is located. These domains probably originated as a result of gene duplication, a proposal supported by their common calcium binding sites and other structural elements [40].

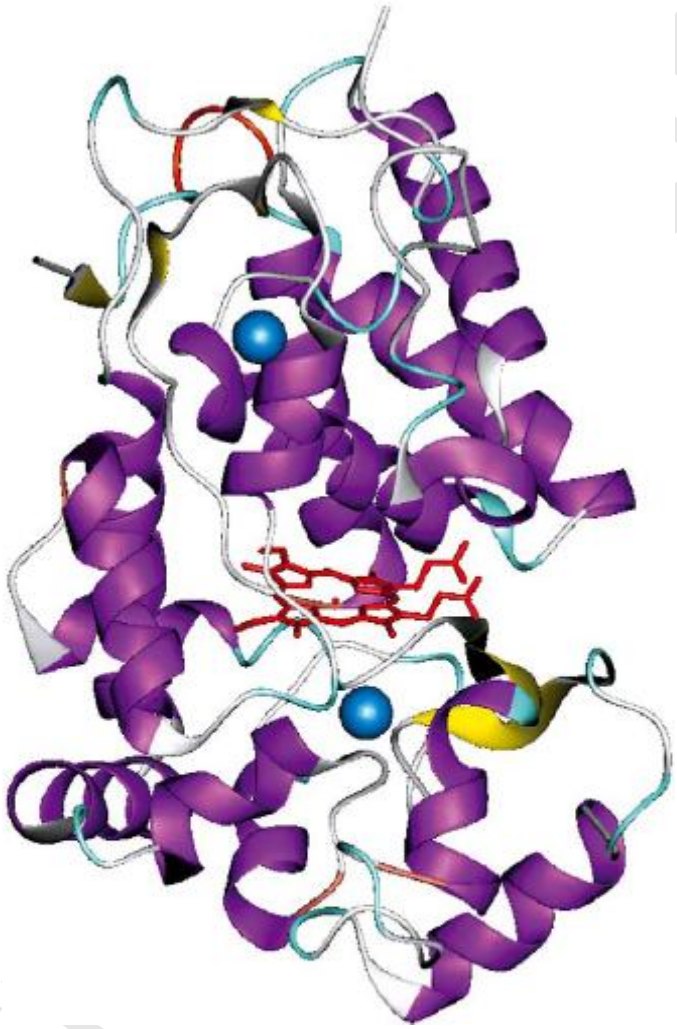

Figure 3.6: *Three-dimensional representation of the X-ray crystal structure of horseradish peroxidase isoenzyme C. The heme group (coloured in red) is located between the distal and proximal domains which each contain one calcium atom (shown as blue spheres). α-Helical and β-sheet regions of the enzyme are shown in purple and yellow, respectively. The F' and F'' α-helices appear in the bottom right-hand quadrant of the molecule [40].*

3.3.2.1.3 HRP catalytic mechanism

The mechanism of catalysis of horseradish peroxidase and in particular, the C isoenzyme, has been investigated extensively. Some important features of the catalytic cycle are illustrated in *Figure 3.7* with ferulic acid as the reducing substrate. The generation of radical species in the two one-electron reduction steps can result in a complex profile of reaction products, including dimers, trimers and higher oligomers that may themselves act as reducing substrates in subsequent turnovers [40].

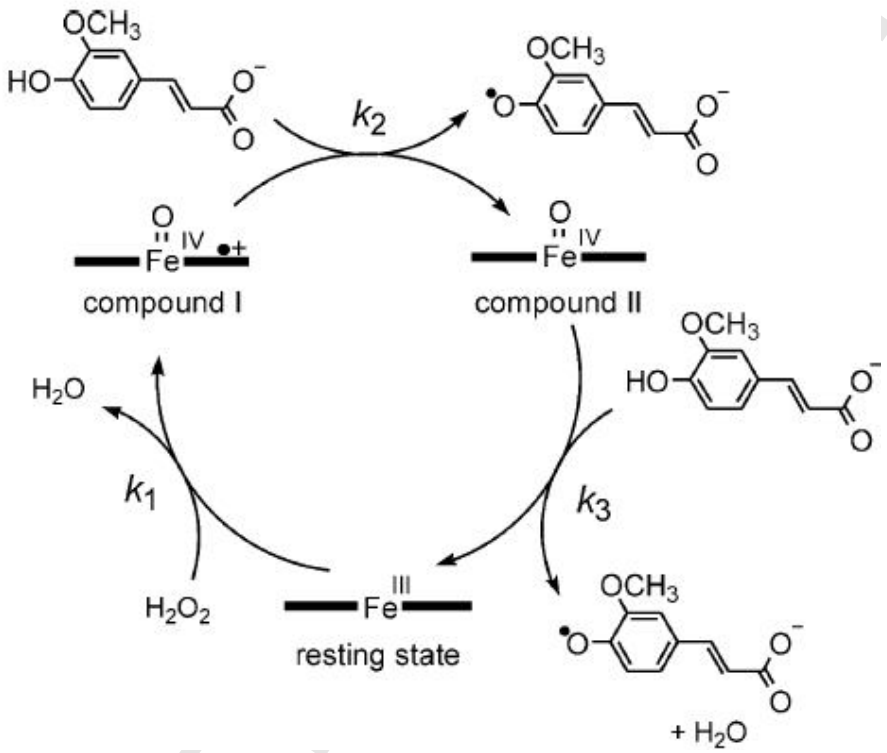

Figure 3.7: *The catalytic cycle of horseradish peroxidase (HRP C) with ferulate as reducing substrate. The rate constants k_1, k_2 and k_3 represent the rate of compound I formation, rate of compound I reduction and rate of compound II reduction, respectively, adapted from [40].*

3.3.2.1.3.1 Formation of Compound I

Different mechanisms for the formation of Compound I have been proposed throughout the years. Nevertheless, the most widely accepted mechanism is based on the model proposed by Poulos and Kraut in 1980 for CcP (*Figure 3.8*) [41]. According to [38], the reaction starts when H_2O_2 enters the heme crevice and binds to the heme iron. This initial interaction between the peroxide and the iron consists in

the formation of a ligand bond between Fe^{III} and one of the peroxide oxygens (the α-oxygen-Oα), and in the subsequent abstraction of a proton by the distal His42 [41]. The intermediate enzyme complex formed is referred in the literature as Compound 0 [41].

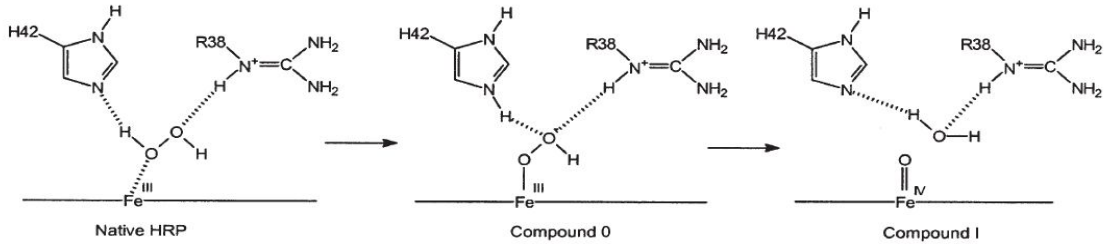

Figure 3.8: *Mechanism of Compound I formation [42].*

This compound is very unstable and has only been detected in cryosolvents at negative temperatures using peroxidase mutants with low activity [43, 44].

The next step consists in the heterolytic cleavage of the O-O bond [41]. His42 transfers the abstracted proton to the β-oxygen (Oβ) and the positively charged guanidinium side chain of Arg38 stabilises the negative charge that is generated at the Oβ, promoting the cleavage of the O-O bond [41]. A water molecule is then produced, while the Oα remains bonded to the heme iron. A fast intramolecular electron transfer then occurs in the heme active site and the oxygen atom acquires two electrons, one withdrawn from the iron and the other from the porphyrin ring [41].

In the mechanism described above, the distal histidine plays the main role as both proton acceptor from Oα and proton donor to Oβ. The distal arginine facilitates the cleavage of the O-O bond. Some authors have proposed the involvement of different residues [45]. If histidine residues are modified with a specific reagent (diethyl pyrocarbonate), the enzyme is still able to reduce H_2O_2 and produce Compound I, while Compound II formation is blocked. It was concluded that His42 was not directly involved in the formation of Compound I and that the carboxylate side chain of Asp43 could participate in the reaction [45].

Recent work suggests that there is no reason to invoke His42 as both proton donor and acceptor [46]. Instead, Arg38 could be the only residue able to donate a proton to

the peroxide Oβ, a mechanism that was supported with molecular dynamics simulation studies.

3.3.2.1.3.2 Formation of Compound I at acidic pH

The formation of Compound I requires the abstraction of a proton from the oxygen bound to the heme iron by a neighbouring residue, a role that has been attributed to the distal histidine [42]. However, at low pH, His42 is protonated and thus cannot accept a proton from the peroxide.

Filizola and Loew proposed that the crystallographic water molecule Wat400 could serve as proton acceptor from the peroxide Oα and that both Arg38 and His42 could play the role of proton donor [46]. They supported the role of Wat400 with the calculated formation of a stable hydrogen bond between the oxygen of this water molecule and the hydrogen in the peroxide Oα.

An alternative mechanism to the one described above, also proposed by Filizola and Loew, is based on a dynamic interchange of the peroxide oxygen atoms as ligands to the heme iron [46]. Loew and colleagues had previously reported that CcP formed a stable complex with HOOH in which the oxygen atoms systematically exchange places as ligands to the iron [47, 48].

The first step in this mechanism is proton donation by Arg38 to the oxygen atom bonded to the iron. Subsequently, the iron ligand changes, allowing the formation of a hydroxywater complex. The water molecule Wat400 then accepts the proton of the ligand oxygen, leading to the formation of the oxywater complex. Rodríguez-López and co-workers presented data that was not consistent with the role of Arg38 as the proton donor at any pH. They suggested a mechanism in which the protonated His42 donates a proton to the peroxide Oβ and further abstracts the proton from the Oα [49].

3.3.2.1.3.3 Mechanism of Compounds I and II reduction

The mechanism of Compounds I and II reduction has not been as intensively studied as the mechanism of Compound I formation. It is generally accepted that when the substrate molecule binds to Compound I, an electron is transferred to the porphyrin ring, via the exposed heme edge, and the π-cation radical disappears [42].

It is also known, from NMR and resonance Raman spectroscopy studies, that this reduction is accompanied by the uptake of a proton, and that this proton does not bind to the oxy-ferryl group.

For the case of a phenolic substrate, the hydrogen bond between Arg38 Nη2 and the phenolic oxygen is thought to assist the proton transfer from the phenol substrate to the protein (*Figure 3.9*) [42]. The final destination of this proton has been suggested to be the imidazole side chain of the distal histidine [42]. As Compound II is formed the radical phenolic substrate leaves the protein and is substituted by a fresh substrate molecule.

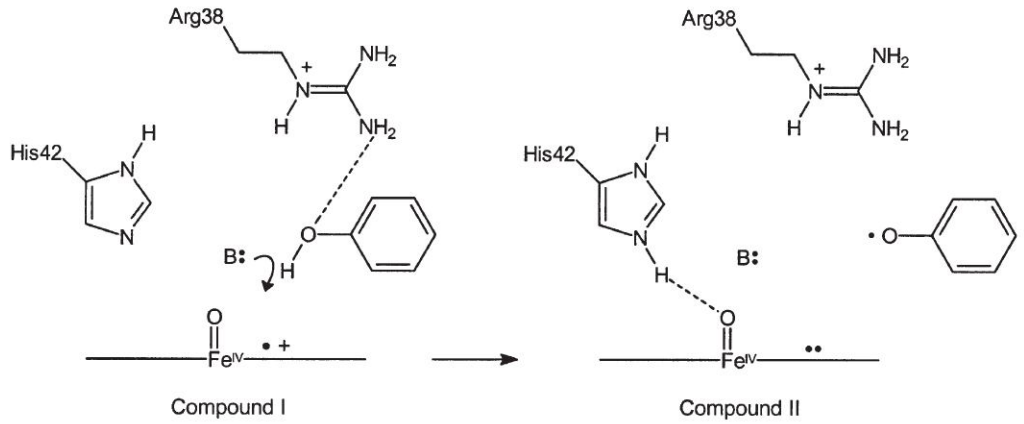

Figure 3.9: *Reduction of Compound I by a phenol substrate molecule. B: represents a protein group that mediates the abstraction of the phenolic proton to His42 [42].*

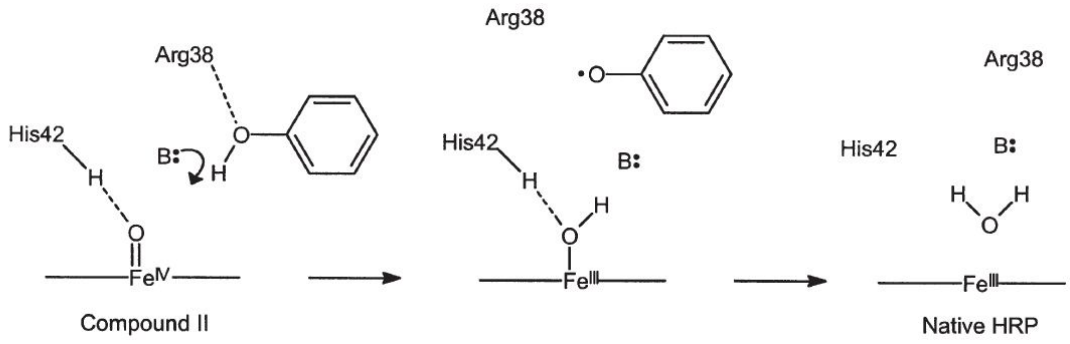

Figure 3.10: *Mechanism of reduction of Compound II [42].*

The reduction of Compound II occurs by a similar mechanism but this time the final destination of both proton and electron is the ferryl oxygen (*Figure 3.10*) [42]. As the ferryl heme iron (Fe^{IV}) is reduced to the ferric state (Fe^{III}), the ferryl oxygen accepts two protons (one from the substrate molecule and the other from the distal His) to form a water molecule that is released from the heme iron [42].

Henriksen and co-workers have suggested that both proton transfer from the substrate molecules could be mediated by a water molecule situated in the active site that is hydrogen bonded to Pro139 [50]. Gajhede proposed a similar mechanism in which the water molecule originated from the peroxide reduction was not removed from the active site and provided the highway for proton transfer [51].

3.3.2.1.4 Applications of HRP in analytical detection

Peroxidases have a considerable potential for application in many different areas. Nevertheless, their commercial application is especially well established in analytical diagnostics, especially, in biosensors and immunodetection.

Horseradish peroxidase (predominantly HRP C) is one of the most widely used enzymes in analytical applications. Due to its characteristics, HRP meets all the requirements for a successful use in analytical systems (e.g. specificity in reaction, flexibility in assay, stability, sensitivity in range of analyte detection, as well as availability in pure form at reasonable cost). Besides that, the ability of HRP to catalyse the oxidation of numerous chromogenic substrates enables the use of spectrophotometric detection systems, including fluorescence and luminescence, opening way to a wide range of procedures. Moreover, the nature of the catalysed reaction (reduction/oxidation reactions) also allows the use of electrochemical detection procedures, and thus the development of electronic biosensors.

Biosensors are becoming more and more important tools in medicine, quality control, food and environmental monitoring and research. There is considerable interest in achieving direct electron transfer between electrodes and proteins for applications to biosensors, chemical synthesis, and fundamental studies. HRP is a prototypical hemeprotein peroxidase, which has been intensively used for determination of H_2O_2. HRP is the most widely studied member of the peroxidase family. Understanding interactions between proteins and surfaces is very important in many fields of biomedical science, from biosensors to biocompatible materials. Protein reconstitution into lipid bilayers has been a particularly useful system for studying the effect of various parameters on protein functionality. Conformational changes of proteins are possible rate-controlling steps in biological electron transfer. The lipid membrane providing biomembrane-like microenvironments are useful for the study of protein redox chemistry, as well as for applications in biosensors and catalysis.

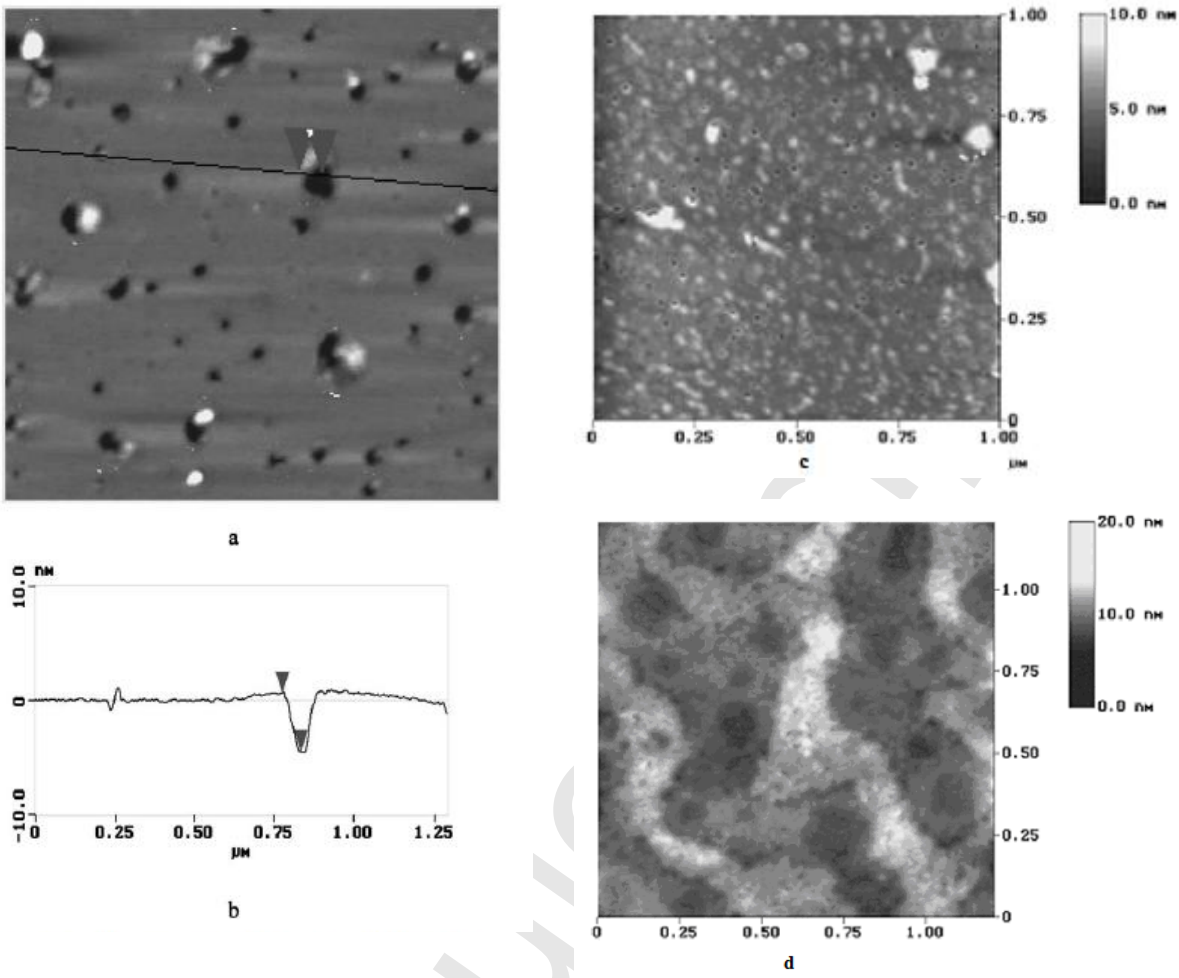

Figure 3.11: *(a) Tapping-mode AFM image of bilayer formed on mica. (b) Height profile along the line shown in (a). The mebrane layer on the mica surface is rather uniform in thickness but contains some defects of pinholes. The shape of most of the defects is circular. (c) Tapping-mode AFM image of HRP absorbed in lipid bilayer. After HRP was deposited on the lipid bilayer, numerous protrusions which were corresponded to HRP molecules in the bilayer films were observed. The defects on the bilayer disappeared. The results indicate that the interaction between the HRP molecular is so strong that the packing of the lipid bilayer is changed. (d) Tapping-mode AFM image of HRP absorbed on bare mica. The image of HRP on the mica surface is not different from that obtained on the HRP-BLM modified mica surface. HRP molecule aggregated together and single HRP molecule could not be seen, adapted from [52].*

Since HRP is capable of reducing H_2O_2 and also some organic peroxides, HRP-based biosensors can be used to control and monitor these peroxides, in pharmaceutical, environmental and dairy industries, in bleaching operations in the textile and paper industries, in air and water ozonisation processes and in food products. The principle of detection is rather simple (*Figure 3.12 and equations 3.1, 3.2*).

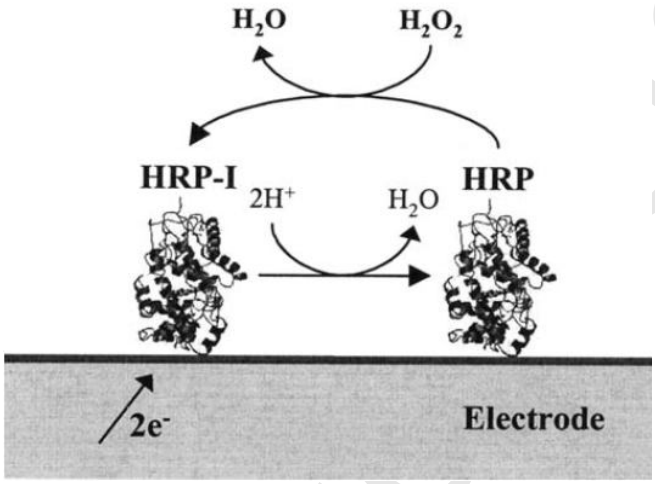

Figure 3.12: *Mechanism of direct electroenzymatic reduction of a peroxide molecule at HRP-modified electrode [42].*

$$\text{Ferric HRP} + H_2O_2 \rightarrow \text{HRP compound I} + 2H_2O \qquad \textit{Eq. 3.1 [53]}$$

$$\text{HRP compound I} + 2e^- + 2H^+ \xrightarrow{\text{electrode}} \text{Ferric HRP} + H_2O \qquad \textit{Eq. 3.2 [53]}$$

If an HRP-modified electrode is placed in a solution containing a peroxide (ROOH) and set at a sufficiently negative potential, then a proportionality between the reduction current and the peroxide concentration is observed (the peroxide oxidises the enzyme and the electrode reduces it back to its native form) [42]. Mediators, small redox molecules (e.g. ferrocene-Fc), can be used to enhance the intensity of the current generated.

3.3.3 Materials and methods

3.3.3.1 Materials

The lipid that was used throughout this study was L-α-phosphatidylcholine from egg yolk (egg PC; Type XVI-E ~ 99% (TLC), Sigma-Aldrich). Silver wire (diameter

1.0 mm) was obtained from Sigma-Aldrich. The enzyme used was Peroxidase, Type XII from Horseradish (1.7 mg solid, Sigma-Aldrich). The hyperoxide solution used was 3% w/w (commercial grade as pharmaceutical preparation; Ecofarm®). All other chemicals were of analytical-reagent grade. Water was distilled through a filtering system (Zalion 300).

3.3.3.2 Biosensor set-up

A two electrode configuration was used throughout the experiments and consisted of a sensing electrode (silver wire with an s-BLM) and an Ag/AgCI electrode acting as a reference. The experimental setup used is shown in *Figures 3.13-3.14*. An external d.c. potential of 25 mV, provided by a power source (model: 2400, SourceMeter® KEITHLEY) was applied between the electrodes and the ionic current through the BLM was measured with a digital electrometer (model: 6514, SYSTEM ELECTROMETER KEITHLEY). The same electrometer was used as a current-to-voltage converter. The electrochemical cell and sensitive electronic equipment were placed in a grounded Faraday cage.

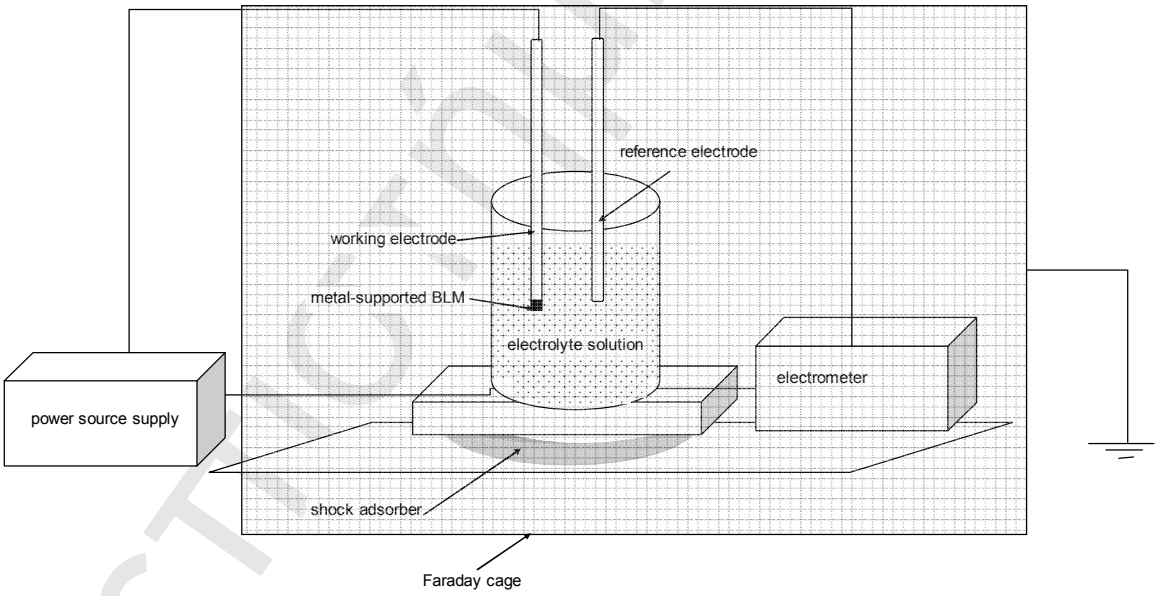

Figure 3.13: *A schematic version of the experimental set-up.*

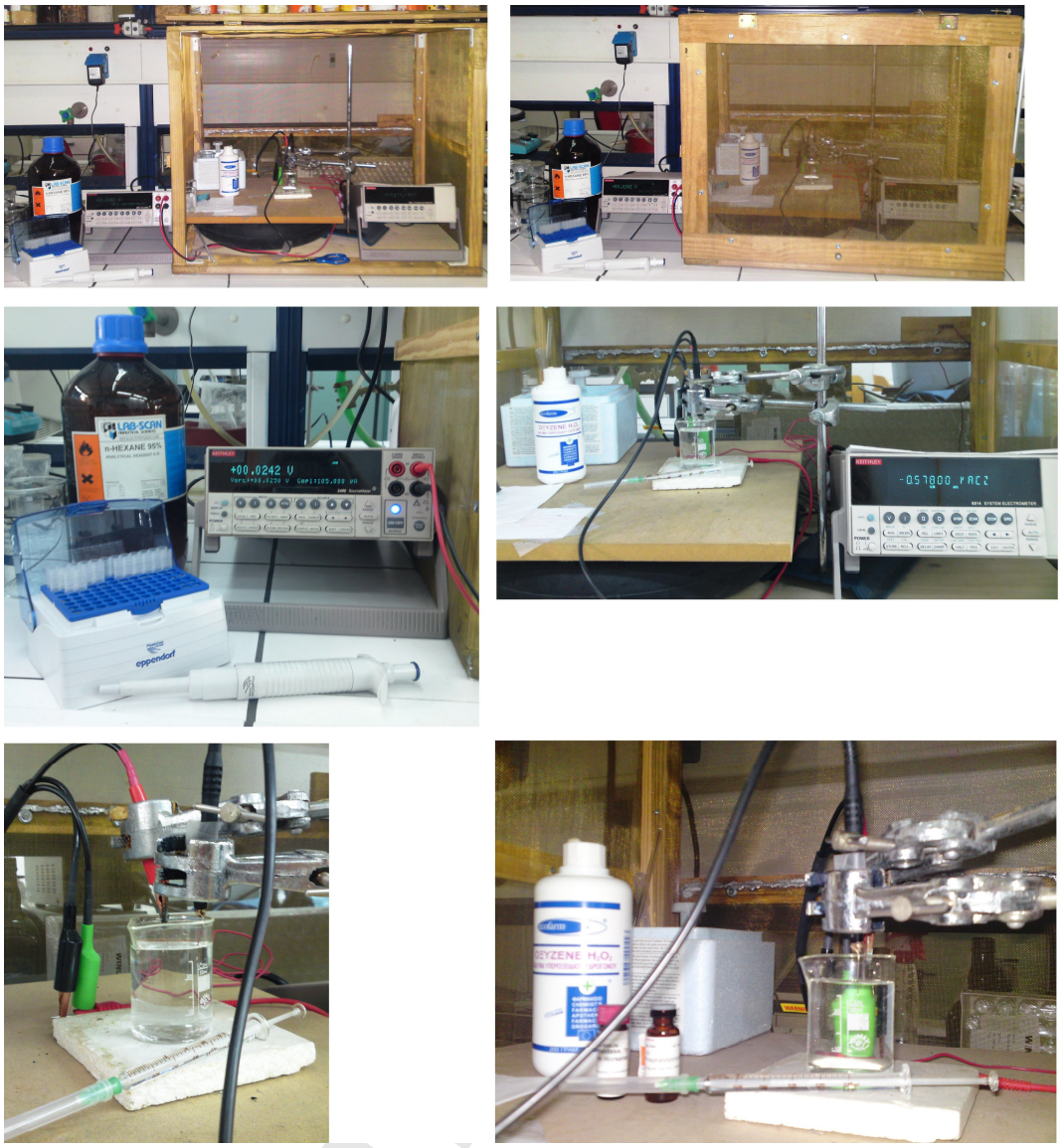

Figure 3.14: *Different views of the cell used for measurements.*

3.3.3.3 Preparation of s-BLMs

The lipid solution used for the formation of the metal supported BLMs contained 2.5 mg/ml of total lipid. The BLMs were supported in a 0.1 M KCI electrolyte solution. s-BLMs were constructed according to the method described in *Section 2.3.1*. A lipid layer was formed onto a nascent metallic surface cut with a scalpel by immersing the metal wire into the lipid solution. The wire coated with the lipid solution was subsequently immersed into a 0.1 M KCI aqueous solution, and the electrochemical current was stabilized over a period of about 22 ± 13 min. All experiments were performed at 20-25 ± 1°C (ambient conditions).

3.3.3.4 Enzyme immobilization

The selectivity of the BLMs towards hydrogen peroxide was obtained by introducing exact concentrations in each experimental procedure of stock horseradish peroxidase solution into the aqueous electrolyte solution, ranging through a decade of concentrations (0.17-1.7 μg/ml). When the ion current stabilized (over a period of ca. 20 min) and no more transient current changes occurred (other than the noise peaks), hydrogen peroxide was injected in the bulk electrolyte solution.

In order to investigate the degree of 'insolubilisation' of the enzyme into the bilayer structure, and possibly to optimize enzyme loading, the lipid forming solution was enriched with 0,34 μg/ml of the enzyme, allowing for both, bilayer formation and enzyme incorporation to proceed in a single step. After the preparation of the mixture, the metal wire, which was freshly cut, was immersed into the mixture. The wire coated with both the lipid solution and the enzyme was subsequently immersed into a 0.1 M KCI aqueous solution. When the ion current stabilized (over a period of 25 ± 5 min) and no more transient current changes occurred (other than the noise peaks), hydrogen peroxide was injected in the bulk electrolyte solution.

3.3.4 Results

3.3.4.1 Stabilisation of BLM

3.3.4.1.1 Stabilisation time of BLM

The mean stabilization time for BLM formation is 22 ± 13 min (n=12), whereas the background current leveled at 120 ± 50 pA and the noise level (estimate) was 33 ± 25 pA. Note that the high variability was due to (i) wiring, (ii) white noise, and (iii) not efficient grounding. The results are presented in *Table 3.1*, whereas a representative current *vs* time diagram is shown in *Diagram 3.1*. An indication of the formation of s-BLMs was given (within one cycle of measurements) by the decrease of the magnitude of the current through the membranes (i.e., from tens of microamperes to picoamperes).

Table 3.1: *Experimental results for stabilization times, background ion currents and noise levels (n=12)*

#	Stabilization times (min)	Background current (pA)	Noise (pA)
1	55	87.63	39.62
2	37	66.26	40.54
3	8	166.40	9.48
4	20	155.30	36.00
5	9	33.20	16.28
6	18	51.00	25.87
7	13	140.30	8.48
8	21	110.11	26.79
9	24	179.64	69.12
10	25	176.06	93.69
11	18	135.45	23.45
12	20	138.57	10.94
Average	**22.33**	**120.00**	**33.35**
Std	**12.84**	**49.93**	**25.58**

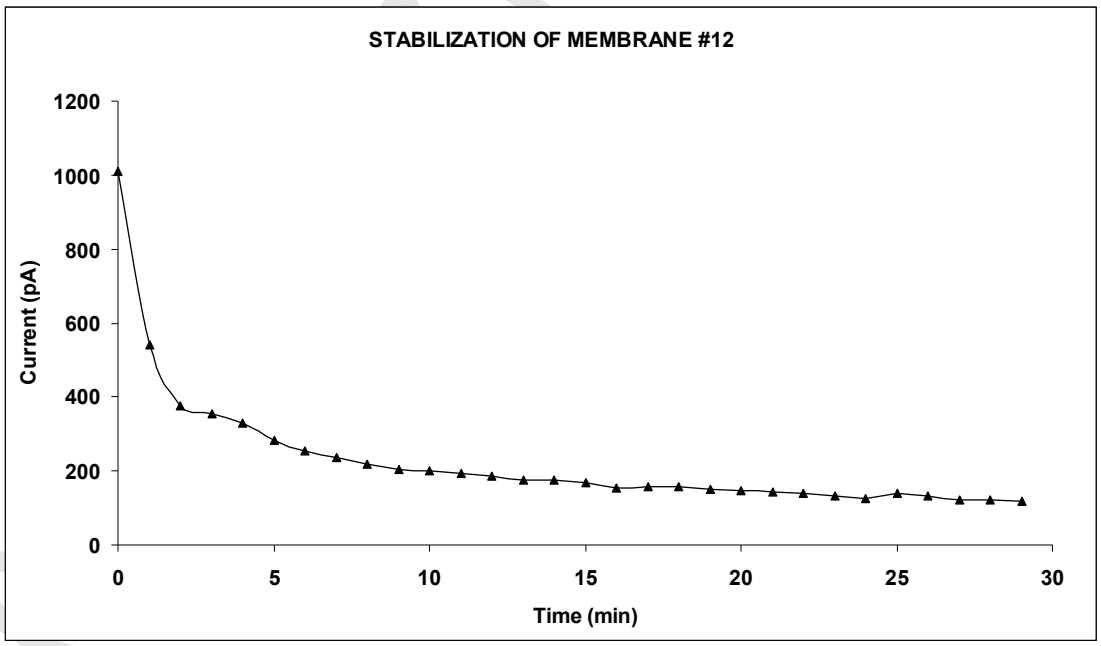

Diagram 3.1: *Stabilization of membrane #12.*

3.3.4.1.2 Breakdown voltage

The breakdown voltage, i.e., the point after which the relation between ion current and voltage becomes non-linear, has been estimated to 105 mV, which is in accordance with values reported for metal supported lipid films from lipid solutions [54], ranging form 100-500 mV. The estimated value, however, is lower than the values reported in the literature for freely supported BLMs (around 350 mV [55]), and even lower than the values given for metal supported BLMs produced in situ by lipid vesicles (around 500 mV, for this type of lipid) [56]. However, a complicated dependence of Young's Modulus and capacitance on the d.c. voltage applied across s-BLM has been reported [26]. The changes of membrane capacitance and of mechanical parameters depend on the polarity of the d.c. voltage, as well as on the direction and rates of change of the dipolar potential, during the decomposition of multilayers into the thickness of a bilayer. It is therefore, not uncommon to produce a less stable structure, although thermodynamically may be proven more favored [55].

3.3.4.1.3 Membrane regeneration

Membrane regeneration *in situ*, i.e., form the lipid solution already present into the electrolyte cell, was not possible, mainly due to the high cell volume (57 ml) used and the consequent high dispersion of the lipid molecules; note that no stirring applied throughout the experiments. Re-forming of membrane was only possible by re-dipping the electrode (after tip-cutting) into the original lipid forming solution.

3.3.4.1.4 Operational stability

Once formed and stabilised, the operational stability of the membrane was satisfactory (95% of the times observed), even at high ambient temperatures (32 ± 2 ^{o}C), although in the latter case, a substantial increase of the noise level was observed. The membrane was stable for over 8 hours (within the experimental runs), showing a drift of 5% in the background ion current after 9 hours of continuous operation.

3.3.4.2 Immobilization of enzyme

3.3.4.2.1 Incorporation of enzyme

The enzyme (5 μl of the stock solution giving a final concentration of 1.7 μg/ml) was injected close to the electrode tip. The injection of the enzyme produced high current transients, indicative of the interaction of the enzyme with the lipid bilayer,

that were gradually reduced after ca. 20 min. The results are presented in *Table 3.2*, whereas a representative ion current *vs* time diagram is shown in *Diagram 3.2*. The average background current was similar to that of a BLM alone, indicating no pore formation of the lipid bilayer. However, the lower noise level, may indicate a less fluid lipid structure, possibly due to surface interaction of the HRP with the membrane; since the egg-PC used in this study is not strongly polar whereas HRP is, these interactions are not due to electrostatic forces between the lipids and the HRP, but rather due to enzyme aggregation at the bilayer surface. If the HRP was spanning the membrane, the background ion current would be expected to increase substantially [38, 52, 57, 58], therefore no deep immersion of the HRP is substantiated, thereby the surface aggregation conclusion is re-enforced.

Table 3.2: *Experimental results for stabilization times, background ion currents and noise levels (n=7) for enzyme incorporation (1.7 μg/ml) into an already formed bilayer.*

#	Stabilization time (min)	Background current (pA)	Noise (pA)
1	21	112.20	22.40
2	21	135.25	12.08
3	14	120.75	17.94
4	13	108.14	21.06
5	21	131.00	8.22
6	15	113.40	16.64
7	13	134.91	15.36
Average	**16.86**	**122.24**	**16.24**
Std	**3.934**	**11.449**	**4.943**

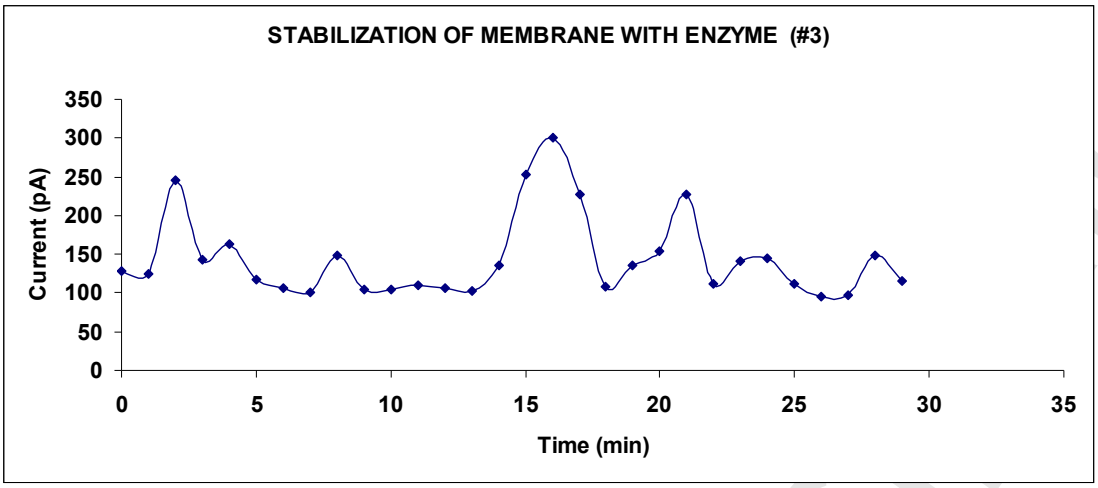

Diagram 3.2: *Stabilization of membrane after enzyme incorporation (1.7 μg/ml).*

The stabilization time was the same at lower concentrations of the enzyme, giving comparable background ion currents. *Table 3.3* presents the results of the incorporation of 0.34 μg/ml, whereas a representative ion current *vs* time diagram is shown in *Diagram 3.3*. It can be noticed, however, a slight increase of the average noise level, as well as a higher variability between the individual values. The use of a lower enzyme concentration (0.17 μg/ml) gave significantly increased noise levels (ca. 50 ± 55 pA), that prohibited any further experimentation. It seems that the lower the concentration of the enzyme the less the aggregation at the membrane surface, but still there is no evidence of membrane spanning or other hydrophobic interaction with the membrane (as monolayer perturbation or flip-flop).

Table 3.3: *Experimental results for stabilization times, background ion currents and noise levels (n=4) for enzyme incorporation (0.34 μg/ml) into an already formed bilayer.*

#	Stabilization time (min)	Background current (pA)	Noise (pA)
1	28	197.00	70.33
2	12	114.85	15.02
3	13	81.670	13.00
4	25	102.11	5.460
Average	**19.50**	**123.9**	**25.95**
Std	**8.185**	**50.61**	**29.87**

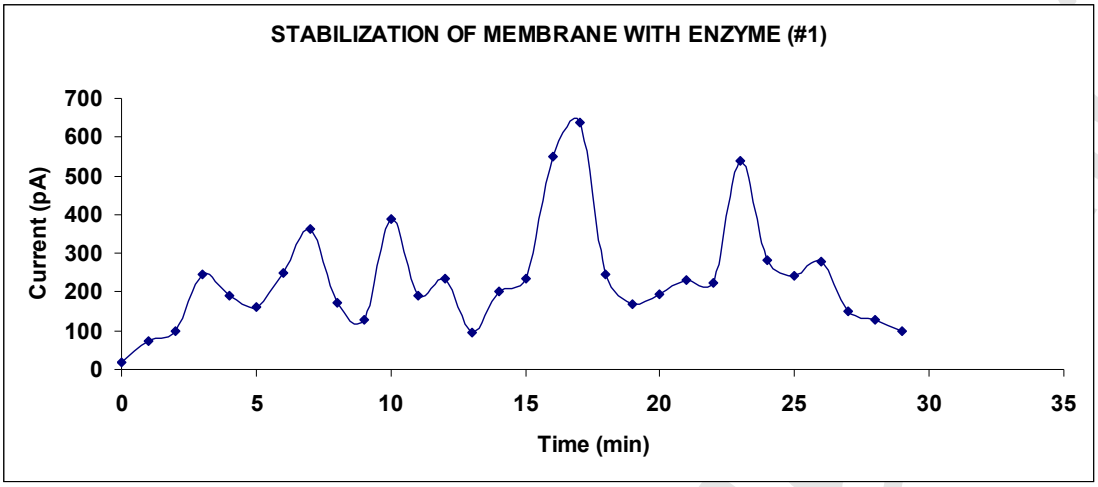

Diagram 3.3: *Stabilization of membrane after enzyme incorporation (0.34 μg/ml).*

The decrease of ion current level over time, indicative of bilayer HRP incorporation (0.34 μg/ml) into the lipid bilayer. The experiment shown is presented in detail in the first row of *Table 3.3*.

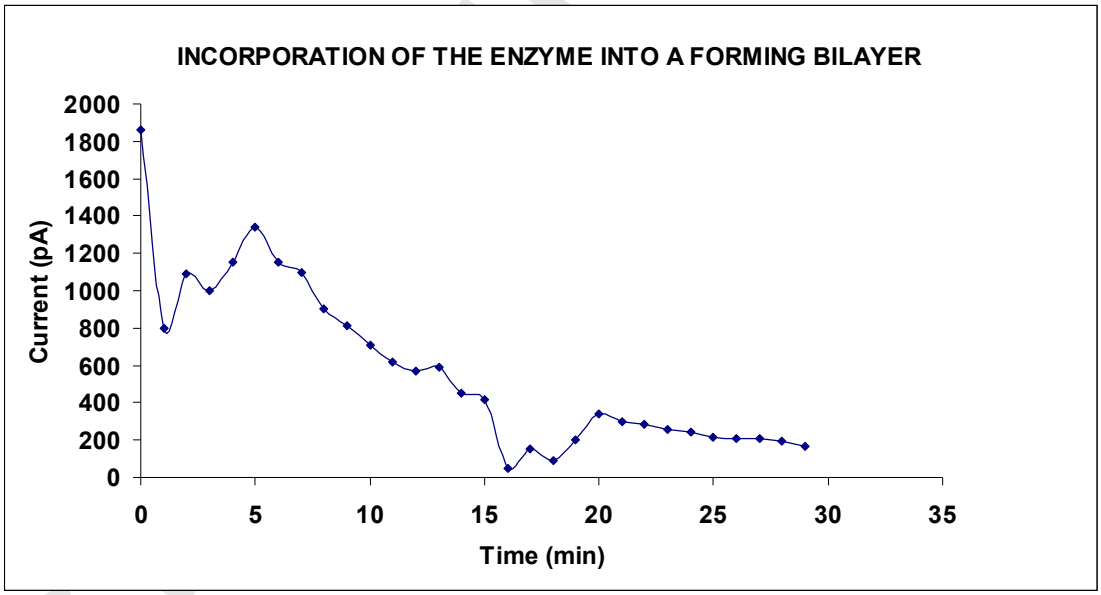

Diagram 3.4: *Simultaneous membrane assembly (2.5 mg/ml) and enzyme (0.34 μg/ml) incorporation.*

The incorporation of enzyme into a forming bilayer gave similar results, with ion current stabilization times of 25 ± 5 min (*Diagram 3.4*). The results indicate that HRP does not span the membrane, supporting the aggregation mechanism. Moreover, the

higher background currents (compared to those obtained when the enzyme incorporated into a pre-formed lipid film) of 240 ± 54 pA (with a noise level of 43.5 pA) suggest limited enzyme diffusion into the bulk electrolyte, making more enzyme available for surface aggregation. Thus, this technique enhances the capacity of the bilayer for enzyme loading at least by a factor of 2.

3.3.4.3 Control experiments

Several control experiments have been performed, including (i) the permeability of the lipid bilayer by the hyperoxide and (ii) the electrochemical detection of the enzymatic reaction in the bulk. It is worthwhile noting that since the pH of the electrolyte solution remains constant throughout the experiments (i.e., 6.5 ± 0.5) it was not necessary to buffer the solution or modify the lipid composition of the membrane.

3.3.4.3.1 Permeability of the lipid bilayer by the analyte

The selectivity of the lipid bilayer to hyperoxide has been studied by injecting hyperoxide concentrations within the range of 0.26 – 1.32 mg/ml into the bulk electrolyte solution. The results have shown that the bilayer exhibits a small response to hyperoxide (*Diagram 3.5*), possibly due to the accumulation of the charged molecules on the bilayer surface that induce a slight increase in the surface charge density of the membrane.

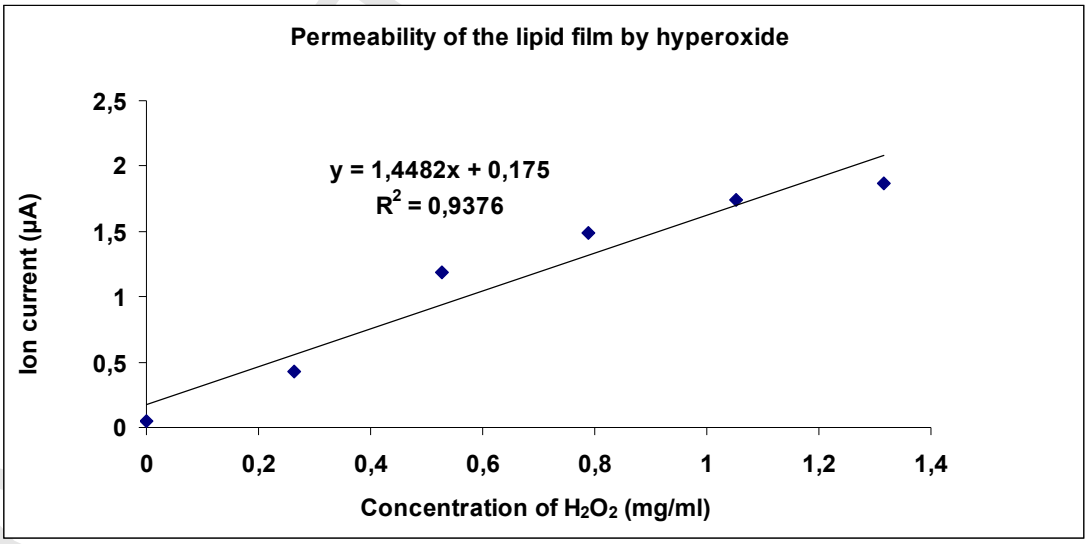

Diagram 3.5: *Permeability of the lipid film by hyperoxide (hyperoxide concentrations within the range of 0.26 - 1.32 mg/ml).*

The response time, on the order of 1 ± 2 s, supports this view, indicating rapid alterations at the membrane surface.

3.3.4.3.2 Electrochemical detection of the enzymatic reaction in the bulk

Potentiometric (against a Ag/AgCl reference electrode) of the HRP – peroxide reaction in the bulk, showed small and irreproducible ion currents, suggesting that the reaction cannot be potentiometrically detected. Since reproducible and relatively high ion currents were achieved by introducing the enzyme into the electrolyte solution after the lipid film thinned to a bilayer structure, it can be concluded that any signal observed is due to electrostatic and/or thermodynamic alterations of the lipid bilayer.

3.3.4.4 Detection of hyperoxide

The introduction of hyperoxide in the bulk electrolyte solution resulted in permanent ion current increases, the magnitude of which depended on the concentration of the analyte (as cumulative concentration levels). The response times (to establish 99% of steady-state current) of a sensor incorporating 1.17 μg/ml of HRP was <1 s. Similar response times have been noticed at lower enzyme concentrations.

The sensor response to hyperoxide concentrations of 0.05 - 1.58 mg/ml, are shown in *Table 3.4*, whereas the calibration curve is provided in *Diagram 3.6*. The analyte was injected as constant μl volume additions (after the appearance of the signal and the stabilization of the system). At any case, the increase of the electrolyte volume in the cell was less than 1%.

Table 3.4: *Sensor response to additions of hyperoxide solution in the bulk electrolyte (enzyme concentration 1.17 μg/ml).*

Final concentration of hyperoxide in the bulk electrolyte (mg/ml)	Average ion current increase (μA)	*n* (no of experiments)	Standard deviation
0.05	0.240	20	0.2369
0.11	0.316	20	0.3304
0.16	0.944	20	0.3838
0.21	2.252	20	1.1858
0.26	2.552	19	2.2660

0.53	8.226	19	3.7622
0.79	17.43	14	4.6345
1.05	23.52	14	6.1577
1.32	27.47	14	5.4198
1.58	35.92	5	2.3616

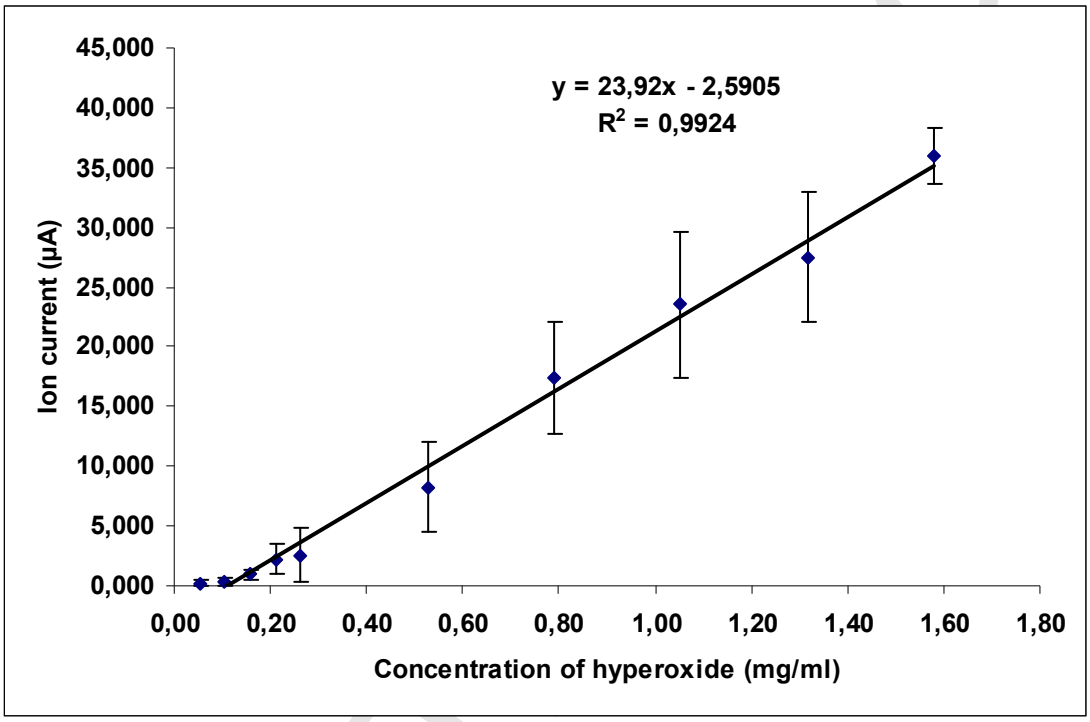

Diagram 3.6: *Calibration Curve. Sensor response to additions of hyperoxide solution in the bulk electrolyte (enzyme concentration 1.17 μg/ml).*

As shown by the calibration curve, the enzyme biosensor offers 20 times more sensitive response than the membrane biosensor alone (see *Section 3.3.4.3.1*). The noise level (i.e., 16.24 pA) sets the detection limit of the sensor (calculated as three times the noise level) at 0.11 mg/ml.

Optimization of analytical signal of the BLM-based sensor toward hyperoxide in 0.1 M KCl electrolyte solution may be achieved by the use of different enzyme concentrations (e.g., 0.34 μg/ml); concentrations of HPR less than 0.34 μg/ml did not provide adequate sensitivity for detection of hyperoxide, i.e., an alteration of current values from ca. 125 to 128 and further to 130 μA occurred when the concentration of hyperoxide increased from 0 to 1.05 mg/ml and further to 1.58 mg/ml respectively,

possibly due to the change in the phase boundary potential; concentrations of HPR greater than 1.17 μg/ml have not been tested.

Table 3.5: *Sensor response to additions of hyperoxide solution in the bulk electrolyte (enzyme concentration 0.34 μg/ml).*

Final concentration of hyperoxide in the bulk electrolyte (mg/ml)	Average ion current increase (μA)	*n* (no of experiments)	Standard deviation
0.053	0.084	9	0.0394
0.105	0.335	10	0.2429
0.158	1.085	14	0.6514
0.211	1.913	15	0.8435
0.263	2.302	15	0.9208

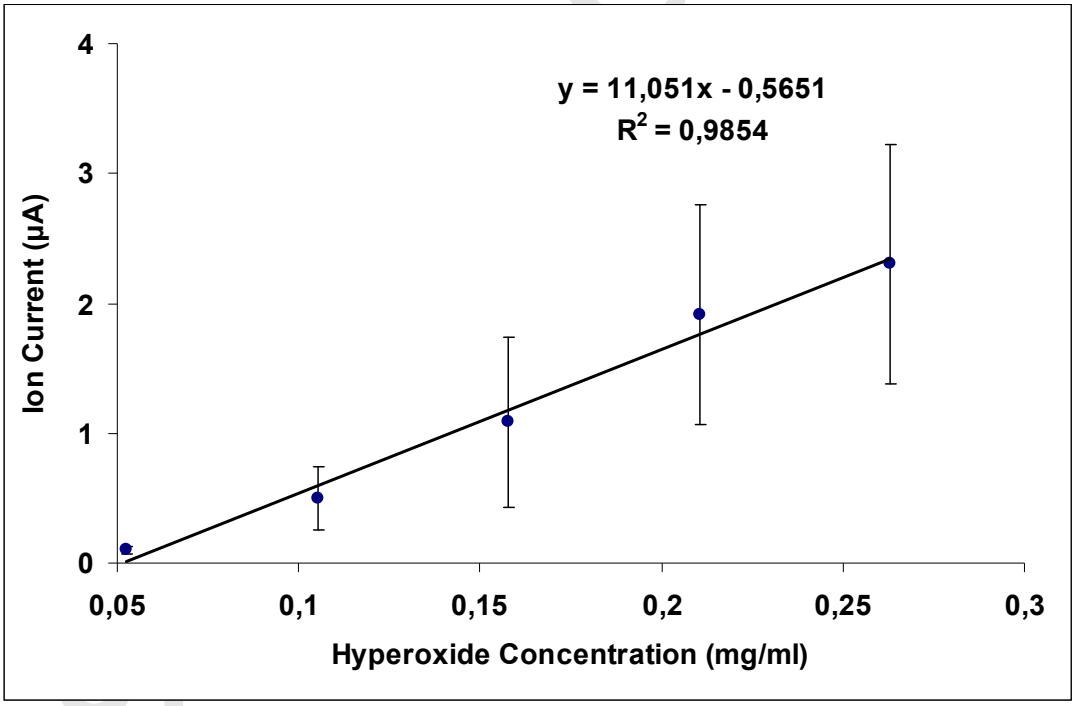

Diagram 3.7: *Calibration Curve. Sensor response to additions of hyperoxide solution in the bulk electrolyte (enzyme concentration 0.34 μg/ml).*

The use of lower concentration of the enzyme (0.34 μg/ml) produced a similar response profile, with permanent ion current increases, the magnitude of which

dependent on the concentration of the analyte in the bulk electrolyre solution. However, the sensitivity of the sensor toward the analyte was much reduced (*Table 3.5* and *Diagram 3.7*) for the high concentration range, but slightly increased for the low concentration range: the noise level (i.e., 25.95 pA) sets the detection limit of the sensor (calculated as three times the noise level) at 0.05 mg/ml.

The use of lipid films incorporating the enzyme during self-assembly (at enzyme concentration of 0.34 μg/ml) produced a similar response profile, with permanent ion current increases, the magnitude of which dependent on the concentration of the analyte in the bulk electrolyte solution. However, the sensitivity of the sensor toward the analyte (for the same enzyme concentration) was slightly increased (*Table 3.6* and *Diagram 3.8*) for the high concentration range, but slightly decreased for the low concentration range: the high noise level (i.e., 43.5 pA) sets the detection limit of the sensor (calculated as three times the noise level) at 0.28 mg/ml.

Table 3.6: *Sensor response to additions of hyperoxide solution in the bulk electrolyte (simultaneous self-assembly and enzyme incorporation; enzyme concentration 0.34 μg/ml).*

Final concentration of hyperoxide in the bulk electrolyte (mg/ml)	**Average ion current increase (μA)**	***n* (no of experiments)**	**Standard deviation**
0.263	8.378	5	3.2584
0.526	18.224	5	2.3182
0.789	20.794	5	5.1512
1.053	25.94	5	4.1693
1.316	29.41	5	5.8278

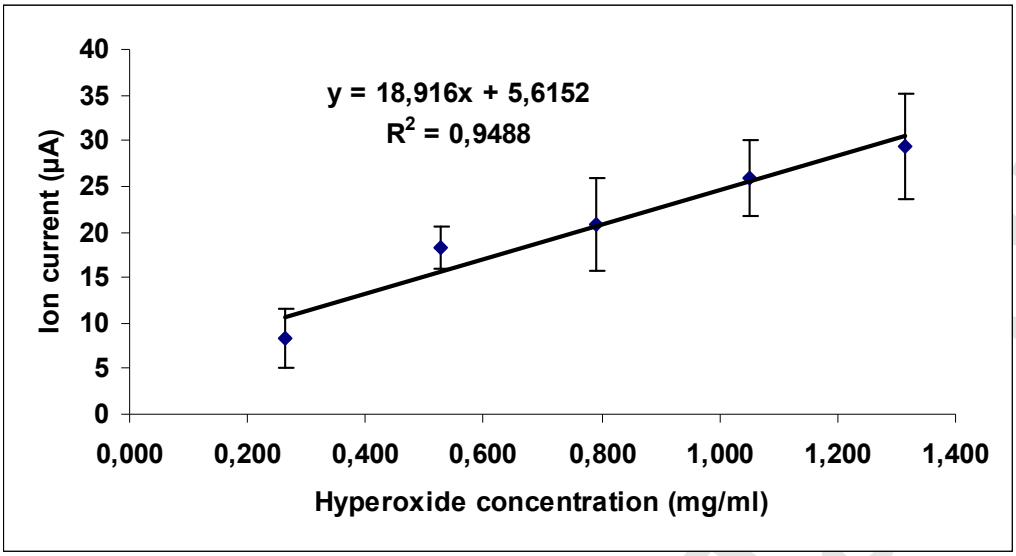

Diagram 3.8: *Sensor response to additions of hyperoxide solution in the bulk electrolyte (simultaneous self-assembly and enzyme incorporation; enzyme concentration 0.34 μg/ml).*

3.3.4.5 Commentary on results

This work describes a technique for the rapid and sensitive electrochemical flow injection monitoring and analysis of hyperoxide using stabilized systems of supported bilayer lipid membranes (s-BLMs) composed of egg phosphatidylcholine (egg PC) with incorporated HRP.

Emfasis was given at the physicochemical part of the analytical development. Results are presented in *Table 3.7*

Table 3.7: *Physicochemical analysis of the membrane.*

Physicochemical analysis of membrane	
Stabilization time (min)	22.33 ± 12.84
Background current (pA)	120 ± 49.93
Noise (pA)	33.35 ± 25.58
Breakdown voltage (mV)	105
Permeability of the lipid film by hyperoxide (C_{H2O2}: 0.26 - 1.32 mg/ml).	$I = 1.4482 \cdot C_{H2O2} + 0.175$ ($R^2 = 0.9376$)

Membrane regeneration *in situ* was not possible, mainly due to the high cell volume. Re-forming of membrane was only possible by re-dipping the electrode (after tip-cutting) into the original lipid forming solution. Once formed and stabilised, the operational stability of the membrane was satisfactory (95% of the times observed). The membrane was stable for over 8 hours (within the experimental runs), showing a drift of 5% in the background ion current after 9 hours of continuous operation. The bilayer shows a small response to hyperoxide, possibly due to the accumulation of the charged molecules on the bilayer surface that induce a slight increase in the surface charge density of the membrane. The response time, on the order of 1 ± 2 s, supports this view, indicating rapid alterations at the membrane surface.

We also examined the physicochemical interaction between the enzyme (HRP) and the membrane. The physicochemical analysis of the interaction between the membrane and the enzyme is described below at *Table 3.8*.

Table 3.8: *Physicochemical analysis of the interaction between membrane - enzyme.*

Physicochemical analysis of the interaction between membrane - enzyme	
Enzyme concentration: 1.17 mg/ml	
Stabilization time (min)	16.86 ± 3.934
Background current (pA)	122.24 ± 11.449
Noise (pA)	16.24 ± 4.943
Enzyme concentration: 0.34 mg/ml	
Stabilization time (min)	19.5 ± 8.185
Background current (pA)	123.9 ± 50.21
Noise (pA)	25.95 ± 29.87

The injection of the enzyme (1.7 μg/ml) produced high current transients, indicative of the interaction of the enzyme with the lipid bilayer, that were gradually reduced after ca. 20 min. The average background current was similar to that of a BLM alone, indicating no pore formation of the lipid bilayer. However, the lower noise level (16.86 ± 3.934 pA), may indicate a less fluid lipid structure, possibly due

to surface interaction of the HRP with the membrane (since the egg-PC used in this study is not strongly polar whereas HRP is) these interactions are not due to electrostatic forces between the lipids and the HRP, but rather due to enzyme aggregation at the bilayer surface. If the HRP was spanning the membrane, the background ion current would be expected to increase substantially, therefore no deep immersion of the HRP is substantiated, and thereby the surface aggregation conclusion is re-enforced. The stabilization time was the same at lower concentrations of the enzyme (0.34 mg/ml), giving comparable background ion currents. It can be noticed, however, a slight increase of the average noise level, as well as a higher variability between the individual values. It seems that the lower the concentration of the enzyme the less the aggregation at the membrane surface, but still there is no evidence of membrane spanning or other hydrophobic interaction with the membrane (as monolayer perturbation or flip-flop). It was also concluded that any signal observed was due to electrostatic and/or thermodynamic alterations of the lipid bilayer since reproducible and relatively high ion currents were achieved by introducing the enzyme into the electrolyte solution after the lipid film thinned to a bilayer structure.

After the analysis of the physicochemical properties of the sensor we studied the ability of the biochemical system to detect H_2O_2 concentrations according to the following reactions.

$$\text{Ferric HRP} + H_2O_2 \rightarrow \text{HRP compound I} + 2H_2O$$

$$\text{HRP compound I} + 2e^- + 2H^+ \xrightarrow{\text{electrode}} \text{Ferric HRP} + H_2O$$

The introduction of hyperoxide in the bulk electrolyte solution resulted in permanent ion current increases, the magnitude of which depended on the concentration of the analyte (as cumulative concentration levels). The response times (to establish 99% of steady-state current) of a sensor incorporating 1.17 μg/ml of HRP was <1 s. The enzyme biosensor offers 20 times more sensitive response than the membrane biosensor alone. The results for the detection of hyperoxide using 1.17 mg/ml enzyme are shown in *Table 3.9*.

Table 3.9: *Detection of hyperoxide using 1.17 mg/ml enzyme.*

Detection of hyperoxide (Hyperoxide concentration: 0.05 - 1.58 mg/ml)	
Enzyme concentration: 1.17 mg/ml	
Response time (sec)	<1
Noise (pA)	16.24 ± 4.943
Detection limit (mg/ml)	0.11
Detection of hyperoxide (C_{H2O2}: 0.05 - 1.58 mg/ml).	$I = 23.92 \cdot C_{H2O2} - 2.5905$ ($R^2 = 0.9924$)

Optimization techniques where also examined including:

a) The use of lower enzyme concentration. Concentrations of HPR less than 0.34 μg/ml did not provide adequate sensitivity for detection of hyperoxide, i.e., an alteration of current values from ca. 125 to 128 and further to 130 μA occurred when the concentration of hyperoxide increased from 0 to 1.05 mg/ml and further to 1.58 mg/ml, possibly due to the change in the phase boundary potential. The use of lower concentration of the enzyme (0.34 μg/ml) produced a similar response profile, with permanent ion current increases, the magnitude of which dependent on the concentration of the analyte in the bulk electrolyre solution. However, the sensitivity of the sensor toward the analyte was much reduced for the high concentration range, but slightly increased for the low concentration range: the noise level (i.e., 25.95 pA) sets the detection limit of the sensor (calculated as three times the noise level) at 0.05 mg/ml. The results for the detection of hyperoxide using 0.34 mg/ml enzyme are shown in *Table 3.10*.

Table 3.10: *Detection of hyperoxide using 0.34mg/ml enzyme.*

Detection of hyperoxide (Hyperoxide concentration: 0.05 – 0.26 mg/ml)	
Enzyme concentration: 0.34 mg/ml	
Response time (sec)	<1

Noise (pA)	25.95 ± 29.87
Detection limit (mg/ml)	0.05
Detection of hyperoxide (C_{H2O2}: 0.05 – 0.26 mg/ml).	$I = 11.051 \cdot C_{H2O2} - 0.5651$ ($R^2 = 0.9854$)

b) Alternative technique of enzyme incorporation from which several conclusions have been drawn indirectly. The incorporation of enzyme into a forming bilayer gave similar results, with ion current stabilization times of 25 ± 5 min. The results indicate that HRP does not span the membrane, supporting the aggregation mechanism. Moreover, the higher residual currents (compared to those obtained when the enzyme incorporated into a pre-formed lipid film) of 240 ± 54 pA (with a noise level of 43.5 pA) suggest limited enzyme diffusion into the bulk electrolyte, making more enzyme available for surface aggregation. Thus, this technique enhances the capacity of the bilayer for enzyme loading at least by a factor of 2. The physicochemical analysis during the incorporation of the enzyme into a forming bilayer is described below at *Table 3.11.*

Table 3.11: *Physicochemical analysis during the incorporation of the enzyme into a forming bilayer.*

Physicochemical analysis during the incorporation of the enzyme into a forming bilayer	
Enzyme concentration: 0.34 mg/ml	
Stabilization time (min)	25 ± 5
Background current (pA)	240 ± 54
Noise (pA)	43.5

The use of lipid films incorporating the enzyme during self-assembly (at enzyme concentration of 0.34 μg/ml) produced a similar response profile in hyperoxide detection, with permanent ion current increases, the magnitude of which dependent on the concentration of the analyte in the bulk electrolyte solution. However, the sensitivity of the sensor toward the analyte (for the same enzyme concentration) was

slightly increased for the high concentration range, but slightly decreased for the low concentration range: the high noise level (i.e., 43.5 pA) sets the detection limit of the sensor (calculated as three times the noise level) at 0.28 mg/ml. The results for the detection of hyperoxide using 0.34 mg/ml enzyme incorporated into a forming bilayer are shown in *Table 3.12*.

Table 3.12: *Detection of hyperoxide using 0.34 mg/ml enzyme incorporated into a forming bilayer.*

Detection of hyperoxide (Hyperoxide concentration: 0.26 – 1.32 mg/ml)	
Enzyme concentration: 0.34 mg/ml	
Response time (sec)	<1
Noise (pA)	43.5
Detection limit (mg/ml)	0.28
Detection of hyperoxide (C_{H2O2}: 0.26 – 1.32 mg/ml).	$I = 18.916 \cdot C_{H2O2} + 5.6152$ ($R^2 = 0.9488$)

4. Discussion and Concluding Remarks

Increases of electrochemical current when s-BLMs were used for detection of commercial hyperoxide solution preparations were obtained within seconds and were indicative of rapid transient alterations of the electrostatic fields and perhaps the internal structural organization of BLMs. Previous studies have examined the interactions of lipophilic molecules (such as atrazine) with dipalmitoylphosphatidyl (DPPC) vesicles using Fourier transform infrared spectroscopy (FT-IR), differential scanning calorimetry (DSC), and fluorescence polarization [59]; the results indicated that lipophilic molecules localize near the glycerol backbone of the lipid without perturbing the hydrophobic core of the lipid bilayer. Differential scanning calorimetry (DSC) studies have shown that alterations of the transition temperature of the vesicular BLMs did occur [60]; these studies have suggested that lipophillic moieties

are involved in hydrogen bonding with the carbonyl groups of the lipid, which is similar to the interactions of other molecules containing hydrogen-bonding donor groups. On the other hand, HRP is mainly a hydrophyllic moiety and it is unlikely to perturb the lipophyllic zone but rather bonds to the polar headgroups at the aquatic interface; moreover, the linear form of the calibration curve (similar for all enzyme concentrations and lipid forming techniques tested herein) does not suggest significant aggregation phenomena.

The present rapid response of s-BLMs to hyperoxide suggests a fast alteration of ion transport through s-BLMs. Lipid membranes composed from phopsphatidylcholine has been proven susceptible to dipolar potential alterations [61] which can be triggered due to the enzyme-analyte interactions at the membrane surface, forming transient pores in the bilayer structure. There were no discernable threshold transients observed during our present experiments using s-BLMs, suggesting that s-BLMs may differ significantly in structure from planar BLMs.

It is possible that the transient signal, which is based on a membrane-charging current, is masked or eliminated by the large ion current through s-BLMs. The pathways for transmembrane ion current could originate from structural defects in the BLM, which would provide transient water-containing pathways capable of salt transport. Whether HRP can alter the very structure of the bilayer is unknown; other commonly proposed mechanisms found in the literature include formation of hexagonal or micellar phase structures that may act as carriers of salts, or lipid flip-flop across BLMs, where the lipid headgroup would be associated with a salt. The short time delay (seconds) for hyperoxide detection when using s-BLMs in comparison to that observed when using planar freely suspended and filter-supported BLMs (minutes) is probably due to structure and mechanism of ion current formation associated with the silver metal electrode that supports s-BLMs. [26]: one side of the s-BLMs (surface of one monolayer) is in contact with the aqueous electrolyte solution; the second monolayer contacts the metal surface, with some regions (depending on the metal roughness) potentially trapping electrolyte solution. The very limited trapped volume of solution makes it possible to reach equilibrium in terms of ion concentration and diffusion very rapidly.

In our experiments, the metal-supported BLMs remained stable for periods of over 48 h. The currents through BLMs stabilized within 22 ± 13 min in average after immersion of the metal wire with the lipid coating into the electrolyte solution

without the analyte. The 22 ± 13 min period required before commencement of measurements when using wire with 1.00 mm diameter is shorter than previously reported times [59]. This is due to the use of PC alone instead of PC mixtures for the preparation of lipid solution. The use of dipalmitoylphoshpatidylecholine mixtures also alters the specific capacitance of s-BLMs from that observed when only PC is used.

The present minisensor responds to increases of hyperoxide concentration in solution and can be suitable for monitoring hyperoxide forming or hyperoxide catalysed reactions. Whether the latter can be feasible remains to be proved by experimentation: increments of electrolyte should be added so as to lower the hyperoxide concentration and observe whether there is a recordable decrease of ion current. For practical applications to sensing, a fresh sensing membrane should be prepared for determination of an unknown sample. This ensures elimination of carryover effects. This also avoids BLM destabilization, which can occur in dry cycling (i.e., transfer of the s-BLM to another electrolyte solution without analyte) due to dehydration of a BLM, or repetitive washing out of hyperoxide after use. The use of freshly prepared s-BLMs is not a serious limitation owing to the simple, inexpensive, and relatively fast method of preparation of this type of sensor. In addition, a number of sensors can be concurrently prepared to compensate for the delay time for s-BLM formation.

In conclusion, the results indicate that hyperoxide can be rapidly screened using the present metal-supported BLM-based minisensor. The approach provides response times of seconds and detection sensitivity and limits for hyperoxide that are suitable for direct analysis of industrial or environmental samples without preconcentration (although sample preparation to eliminate other adsorbents to BLMs may be necessary). While the work presented here represents an attractive configuration and application of electrochemistry of BLM-based sensors, the practical use of such a sensor for real world applications needs to be further researched for robustness, lifetime, manufacturability, and other performance requirements that will further allow commercialization of the present device.

References

1. C.G. Siontorou, F.A. Batzias, *Ecological Indicators*, **11,** 564-581, (2011).
2. A.F. Batzias, C.G. Siontorou, *Journal of Hazardous Materials*, **158**, 340-358, (2008).
3. C.G. Siontorou, F.A. Batzias, *Critical Reviews in Biotechnology*, **30**, 79-86, (2010).
4. D.R. Thévenot, K. Toth, R.A. Durst, G.S. Wilson, *Biosensors Bioelectronics,* **16**, 121-131 (2001).
5. K.A. Fähnrich, *PhD thesis in Analytical Chemistry*, Ireland (2002), http://www.karstenfaehnrich.de/PhD_Karsten_final__links_.pdf
6. A. Hulanicki, S. Glab, F. Ingman, *Pure and Applied Chemistry*, **63**, 1247-1250 (1991).
7. D. van der Lelie, P. Corbisier, W. Baeyens, S. Wuertz, L. Diels, M. Mergeay, *Research in Microbiology*, **145**, 67-82, (1994).
8. W.S. Kisaalita, *Biosensors & Bioelectronics*, **7,** 613-620, (1992).
9. S. Sethi, *Biosensors & Bioelectronics*, **9**, 243-264, (1994).
10. J.P. Salvador, J. Adrian, R. Galve, D.G. Pinacho, M. Kreuzer, F. S. Baeza, M.P. Marco, *Comprehensive Analytical Chemistry*, **50**, 279-334, (2007).
11. R. Lal, *Bioelectrochemistty and Bioenergetics,* **27**, 121-139, (1992).
12. B.M. Paddle, *Biosensors & Bioelectronics*, **11**, 1079-1113, (1996).
13. M. P. Byfield, R. A. Abuknesha, *Biosensors & Bioelectronics*, **9**, 373-400, (1994).
14. F.R.R. Teles, L.P. Fonseca, *Talanta*, **77**, 606-623, (2008).
15. J. Li-Fries, *PhD thesis in Sciense*, Mainz (2007), http://www.mpip-mainz.mpg.de/groups/knoll/Publication/theses/2007/lifries_2007
16. A.L. Ottova, H.T. Tien, *Bioelectrochemistry and Bioenergetics*, **42**, 141-152, (1997).
17. D.J. Woodbury, *Journal of Membrane Biology*, **109**, 145-150, (1989).
18. F. Davis, S.P.J. Higson, *Biosensors and Bioelectronics*, **21**, 1–20, (2005).
19. I. Langmuir, *Journal of the American Chemical Society*, **39**, 1848-1906, (1917).
20. K.B. Blodgett, *Journal of the American Chemical Society*, **57**, 1007-1022, (1935).
21. A. Ottova-Leitmannova, H.T. Tien, *Progress in Surface Science*, **41**, 337-445, (1992).
22. A. Ottova, H.T. Tien, *Advances in Planar Lipid Bilayers and Liposomes*, **1**, 1-76, (2005).

23. A. Ottova, V. Tvarozek, J. Racek, J. Sabo, W. Ziegler, T. Hianik, H.T. Tien, *Supramolemlar Science*, **4**, 101-112, (1997).
24. K.L. Mittal (Ed.), *Plenum Press, New York*, **8**, 133, (1989).
25. Kuang-Lee Chiang, U.J. Krull, D.P. Nikolelis, *Analytica Chimica Acta*, **357**, 73-77, (1997).
26. T. Hianik, V.I. Passechnik, D.F. Sargent, J. Dlugopolsky, L. Sokolikova, *Bioelectrochemistry and Bioenergetics*, **37**, 61-68 (1995).
27. A. E. Filonov, W. A. Duetz, A. V. Karpov, R. R. Gaiazov, I. A. Kosheleva, et al., *Applied Microbiology and Biotechnology*, **48**, 493-498, (1997).
28. A.N. Reshetilov, P.V. Iliasov, A.E. Filonov, R.R. Gayazov, I.A. Kosheleva, A.M. Boronin, *Process Biochemistry*, **32**, 487-493, (1997).
29. J.D. Van Hamme, A. Singh, O.P. Ward, *Microbiology and Molecular Biology Reviews*, **67**, 503-549, (2003).
30. G.I. Paton, B.J. Reid, K.T. Semple, *Environmental Pollution*, **157**, 1643-1648, (2009).
31. R.M.H. Merks, J.A. Glazier, *Physica A: Statistical Mechanics and its Applications*, **352**, 113-130, (2005).
32. W. Zhang and G. Li, *Analytical Sciences*, **20**, 603-609, (2004).
33. L. Gorton, G. Jönsson-Pettersson, E. Csöregi, K. Johansson, E. Dominguez, G. Marko-Varga, *Analyst*, **117**, 1235-1241, (1992).
34. T. Ruzgas, E. Csöregi, J. Emnéus, L. Gorton, G. Marko-Varga, *Analytica Chimica Acta*, **330**, 123-138, (1996).
35. A.L. Ghindilis, P. Atanasov, E. Wilkins, *Electroanalysis*, **9**, 661-674, (1997).
36. C. Petit, K. Murakami, A. Erdem, E. Kilinc, G.O. Borondo, J.F. Liegeois, J.M. Kauffmann, *Electroanalysis*, **10**, 1-8, (1998).
37. S. Yang, Y. Li, X. Jiang, Z. Chen, X. Lin, *Sensors and Actuators B*, **114**, 774-780, (2006).
38. K. Chattopadhyay, S. Mazumdar, *Biochemistry*, **39***,* 263-270, (2000).
39. P.J. O'Brien, *Chemico-Biological Interactions*, **129**, 113-139, (2000).
40. N.C. Veitch, *Phytochemistry*, **65**, 249-259, (2004).
41. T.L**.** Poulos, S.T. Freer, R.A. Alden, S.L. Edwards, U. Skogland, K. Takio, B. Eriksson, N. Xuong, T. Yonetani, J. Kraut, *Journal of Biological Chemistry*, **255**, 575-580, 1980.

42. A.M. Azevedo, V.C. Martins, D.M.F. Prazeres, V. Vojinović, J.M.S. Cabral, L.P. Fonseca, *Biotechnology Annual Review*, **9**, 199-247, (2003).
43. H.K. Baek, H.E. Van Wart, *Journal of the American Chemical Society*, **114**, 718-725, (1992).
44. J.N. Rodriguez-Lopez, A.T. Smith, R.N.F. Thorneley, *Journal of Biological Chemistry*, **271**, 4023-4030, (1996).
45. D.Kr. Bhattacharyya, U. Bandyopadhyay, R.K. Banerjee, *Journal of Biological Chemistry*, **268**, 22292-22298, (1993).
46. M. Filizola, G.H. Loew, *Journal of the American Chemical Society*, **122**, 18-25, (2000).
47. D.L. Harris, G.H. Loew, *Journal of the American Chemical Society*, **118**, 10588-10594, (1996).
48. G. Loew, M. Dupuis, *Journal of the American Chemical Society*, **118**, 10584-10587, (1996).
49. J.N. Rodríguez-López, D.J. Lowe, J. Hernández-Ruiz, A.N.P. Hiner, F. García-Cánovas, R.N.F. Thorneley, *Journal of the American Chemical Society*, **123**, 11838-11847, (2001).
50. A. Henriksen, A.T. Smith, M. Gajhede, *Journal of Biological Chemistry*, **274**, 35005-35011, (1999).
51. M. Gajhede, *Biochemical Society Transactions*, **29**, 91-99, (2001).
52. J. Tang, J. Jiang, Y. Song, Z. Peng, Z. Wu, S. Dong, E. Wang, *Chemistry and Physics of Lipids*, **120**, 119-129, (2002).
53. S.S. Razola, B.L. Ruiz, N.M. Diez, H.B. Mark, Jr, J.M. Kauffmann, *Biosensors and Bioelectronics*, **17**, 921-928, (2002).
54. T. Hianik, J. Dlugopolsky, M. Gyepessova, *Bioelectrochemistry and Bioenergetics*, **31**, 99-111, (1993).
55. D.S. Dimitrov, R.K.Jain, *Biochimica et Biophysica Acta*, **779**, 437-468, (1984).
56. H.T. Tien, S.H. Wurster, A.L. Ottova, *Bioelectrochemistry and Bioenergetics*, **42**, 77-94, (1997).
57. J. Zhao, R.W. Henkens, J. Stonehuerner, J.P. O'Daly, A.L. Crumbliss, *Journal of Electroanalytical Chemistry*, **327**, 109-119, (1992). ΑΠΟ AFM
58. J.F. Rusling, A.E.F. Nassar, , *Journal of the American Chemical Society*, **115**, 11891-11897, (1993).
59. C.G. Siontorou, D.P. Nikolelis, *Analytical Chemistry*, **69**, 3109-3114, (1997).

60. D. P Nikolelis, C.G. Siontorou, *Electroanalysis*, **8**, 907-912, (1996).
61. D. P Nikolelis, C.G. Siontorou, *Analytical Chemistry*, **67**, 936-944, (1995).